Species-specific quorum sensing represses the chitobiose utilization locus in *Vibrio cholerae*

Catherine A. Klancher, Jane D. Newman, Alyssa S. Ball, Julia C. van Kessel, and Ankur B. Dalia*

Department of Biology, Indiana University, Bloomington, IN 47405
*Author for correspondence: ankdalia@indiana.edu

Abstract

The marine facultative pathogen *Vibrio cholerae* forms complex multicellular communities on the chitinous shells of crustacean zooplankton in its aquatic reservoir. *V. cholerae*-chitin interactions are critical for the growth, evolution, and waterborne transmission of cholera. This is due, in part, to chitin-induced changes in gene expression in this pathogen. Here, we sought to identify factors that influence chitin-induced expression of one locus, the chitobiose utilization operon (*chb*), which is required for the uptake and catabolism of the chitin disaccharide. Through a series of genetic screens, we identified that the master regulator of quorum sensing, HapR, is a direct repressor of the *chb* operon. We also found that the levels of HapR in *V. cholerae* are regulated by the ClpAP protease. Furthermore, we show that the canonical quorum sensing cascade in *V. cholerae* regulates *chb* expression in a HapR-dependent manner. Through this analysis we found that signaling via the species-specific autoinducer CAI-1, but not the inter-species autoinducer AI-2, influences *chb* expression. This phenomenon of species-specific regulation may enhance the fitness of this pathogen in its environmental niche.

Importance

In nature, bacteria live in multicellular and multispecies communities. Microbial species can sense the density and composition of their community through chemical cues using a process called quorum sensing (QS). The marine pathogen *Vibrio cholerae* is found in communities on the chitinous shells of crustaceans in its aquatic reservoir. *V. cholerae* interactions with chitin are critical for the survival, evolution, and waterborne transmission of this pathogen. Here, we show that *V. cholerae* uses QS to regulate the expression of one locus required for *V. cholerae*-chitin interactions.

Introduction

The facultative bacterial pathogen *Vibrio cholerae*, the causative agent of the diarrheal disease cholera, natively resides in the aquatic environment. In this niche, *V. cholerae* forms multicellular communities on biotic and abiotic chitinous surfaces, like the shells of crustaceans or marine snow (1, 2). Chitin is a polysaccharide made up of β-1,4 linked *N*-acetylglucosamine (GlcNAc) and serves as a major nutrient source for *V. cholerae* in the marine environment (1, 3, 4). The ability of *V. cholerae* to form chitin biofilms is critical for the waterborne

transmission of cholera (5, 6). As chitin is the most abundant biopolymer in the ocean, the ability of *Vibrio* species to break down and utilize this highly insoluble polysaccharide also serves an important role in global nitrogen and carbon recycling (1, 4).

When *V. cholerae* is associated with a chitinous surface, chitin induces the expression of a subset of genes in *V. cholerae*. The genes induced by chitin include those required for chitin degradation, uptake, and catabolism (termed the chitin utilization program), as well as the genes required for natural transformation (7, 8). Transcriptional responses resulting from *Vibrio*-chitin interactions are highly regulated. One major chitin-responsive regulator is the orphan hybrid sensor kinase ChiS (7, 9). ChiS senses chitin indirectly through the periplasmic chitin binding protein (CBP) (9, 10). In the absence of chitin, CBP represses ChiS through interactions with its periplasmic domain (9, 10). In the presence of chitin, the CBP-chitin complex stimulates ChiS activity (9, 10). Thus, in the presence of chitin, ChiS is active and can facilitate expression of the chitin utilization program. Alternatively, ChiS can be genetically activated in the absence of chitin by deleting *cbp* (10, 11).

In the marine environment, *V. cholerae* not only senses chitin to modulate gene expression, but also the presence of other bacteria through a process termed “quorum sensing” (QS) (12). This is a process by which bacteria indirectly sense other microbes in their community via small diffusible molecules called autoinducers (AIs). AIs are sensed by cognate sensor proteins. *V. cholerae* encodes four AI sensors, although the autoinducer molecules that serve as inducing cues are only known for two of them (13). AI sensing allows for cell-density specific gene expression programs, which regulate “group” or “individual” behaviors (14). *V. cholerae* senses both chitin and AIs to regulate natural transformation on chitinous surfaces (15). Though a link between chitin utilization and quorum sensing has previously been suggested, it has not been directly studied (16).

To investigate regulation of the chitin utilization program in *V. cholerae*, most studies employ the chitobiose utilization operon (*chb*) (10, 11, 17, 18). The *chb* operon encodes the genes required for uptake and catabolism of the chitin disaccharide chitobiose, and is highly induced in the presence of chitin oligosaccharides (7). Several mechanisms of *chb* regulation have already been identified. ChiS is the master regulator of the chitin utilization program in *V. cholerae*, and we have recently shown this protein is a direct transcriptional activator required for induction of the *chb* locus (9, 10). Previous work has shown that carbon catabolite repression (CCR) can also play a role in regulating chitin responsive phenotypes including ChiS-dependent induction of *chb* and natural transformation (18, 19). In addition, our group has previously found that the cell division licensing factor SlmA plays an essential role in activating *chb* expression (11). Tight regulation via these diverse signaling systems may act to ensure that

the chitin utilization program is only expressed under conditions in which it will provide a competitive advantage.

Here, we sought to identify additional regulators of *chb*. Through a number of genetic screens and complementary molecular methods, we show that quorum sensing is an additional regulatory system that tunes expression of a chitin utilization locus in *V. cholerae*.

Results

ClpA is identified in an unbiased screen for activators of P_{chb}

To identify additional genes required for activation of the *chb* locus, we conducted a transposon mutant screen. This was carried out in a strain containing a chromosomally-integrated P_{chb}-*lacZ* transcriptional reporter. As shown previously, induction of P_{chb} is dependent on the activity of the master regulator ChiS (7, 10, 11). In the absence of chitin, ChiS activity is repressed by CBP. In the presence of chitin, CBP repression of ChiS is relieved, which allows for ChiS-dependent activation of P_{chb}. In addition to being induced by chitin, ChiS can be activated genetically in the absence of chitin by deleting *cbp* (10, 11). As chitin oligomers are prohibitively expensive, a Δ*cbp* mutation was used to induce ChiS-dependent P_{chb}-*lacZ* expression in our genetic screen exactly as previously described (11). So, the starting genotype for our screen was a strain containing P_{chb}-*lacZ* and a Δ*cbp* mutation. This strain formed blue colonies on X-gal containing plates and we screened for white colonies to identify putative activators that contribute to P_{chb} induction.

Of approximately 60,000 transposon mutants visually screened for loss of P_{chb}-*lacZ* expression, one gene identified was *clpA* (2 unique transposon insertions). Other hits identified in this screen are listed in **Table S1**. To study the effect of *clpA* on P_{chb} activity moving forward, we utilized a previously described chromosomally-integrated P_{chb}-GFP reporter (10, 11). Using this reporter, we found that a Δ*clpA* mutation resulted in a ~3-fold decrease in P_{chb} expression relative to the parent (**Fig. 1**). Importantly, complementation of this strain with an ectopic copy of *clpA in trans* restored P_{chb} expression to parent levels (**Fig. S1**). ClpA is a AAA+ unfoldase that recognizes protein substrates, unfolds them, and feeds them into the ClpP protease where they are degraded (20). If ClpA was exhibiting its effect on P_{chb} expression as a part of the ClpAP machine, we hypothesized that a Δ*clpP* mutation should phenocopy a Δ*clpA* mutation. Indeed, Δ*clpP* and Δ*clpP* Δ*clpA* strains phenocopied a Δ*clpA* mutant for P_{chb} expression (**Fig. 1**). These results suggest that loss of the ClpAP protease decreases P_{chb} expression. As ClpAP degrades proteins, we hypothesized that ClpAP may indirectly promote activation of P_{chb} by degrading a repressor of the *chb* locus.

HapR is a repressor of P_{chb} that is degraded by ClpAP

To identify a putative repressor of P_{chb} that is targeted by ClpAP for degradation, we conducted a counter-screen using the P_{chb}-*lacZ* reporter. For the Δ*clpA* counter-screen, the parent strain had both Δ*cbp* and Δ*clpA* mutations. This

138 mutant is white on X-gal plates because P_{chb}-*lacZ* is poorly expressed;
139 inactivation of the putative repressor in this strain should result in restoration of
140 P_{chb}-*lacZ* expression and yield a blue colony phenotype. In the Δ*clpA* counter-
141 screen, we visually screened approximately 30,000 transposon mutants for re-
142 activation of P_{chb}-*lacZ* expression and identified *hapR* (9 unique transposon
143 insertions). Other hits identified in this screen are listed in **Table S1**. A Δ*hapR*
144 mutation restored P_{chb} expression in the Δ*clpA* mutant background (**Fig. 1**). In
145 fact, a Δ*hapR* mutation allowed for higher P_{chb} expression than the parent strain.
146 This suggests that HapR represses P_{chb} expression when ClpAP is intact and
147 that ClpAP does not degrade the entire pool of HapR in the cell (**Fig. 1**).
148 Importantly, the level of P_{chb} expression observed in the Δ*hapR* Δ*clpA* mutant
149 phenocopied the Δ*hapR* strain (**Fig. 1**). This epistasis between *clpA* and *hapR*
150 suggests that they are involved in the same pathway for regulating P_{chb}
151 expression. In addition, complementation of the Δ*hapR* strain with an ectopic
152 copy of *hapR in trans* decreased P_{chb} expression almost to the level in the parent
153 (**Fig. S1**). Further, complementation of the Δ*hapR* Δ*clpA* strain with *hapR in trans*
154 brought P_{chb} expression down to the level observed in the Δ*clpA* parent (**Fig. S1**).
155
156 We hypothesized that the reason P_{chb} expression was decreased in Δ*clpAP*
157 mutants was due to increased HapR protein levels. Western blotting in these
158 backgrounds revealed that HapR levels were, indeed, increased in strains
159 containing mutations to *clpA* and/or *clpP* (**Fig. 1**). ClpAP dependent degradation
160 of HapR is not unique to *V. cholerae*, but has previously been observed in *Vibrio*
161 *vulnificus* where ClpAP degrades the HapR homolog SmcR (21). In addition to
162 the ClpAP machine, it was shown that the Lon protease also plays a role in
163 SmcR degradation. So, we next sought to investigate the role of other protease
164 machines on induction of P_{chb} and HapR protein levels. Mutations to other Clp
165 components (the ClpS adaptor protein or the ClpX unfoldase*)* did not have a
166 marked impact on HapR protein levels. Also, a Δ*clpS* mutation did not affect P_{chb}
167 expression levels, while a Δ*clpX* mutation slightly decreased P_{chb} expression
168 (**Fig. 1**). Because HapR expression was not affected by the Δ*clpX* mutation, the
169 observed decrease in P_{chb} expression may be attributed to a pleiotropic effect
170 (*i.e.*, an effect of *clpX* that is independent of HapR-dependent P_{chb} repression). In
171 contrast to the effect of the Lon protease on SmcR levels in *V. vulnificus*, we did
172 not observe an impact of Δ*lonA* on HapR levels in *V. cholerae*; and Δ*lonA*,
173 correspondingly, did not affect P_{chb} expression (**Fig. 1**). Together, these results
174 establish that HapR is a repressor of P_{chb} and that HapR levels are controlled
175 specifically by the ClpAP protease in *V. cholerae*.
176
177 *HapR-mediated repression of P_{chb} occurs on chitinous surfaces*
178 Thus far, we have studied P_{chb} regulation using a Δ*cbp* mutation to induce ChiS
179 activity. Natural induction of this locus, however, occurs in the presence of chitin
180 oligosaccharides. So, we next wanted to test whether the repression of P_{chb} by
181 HapR was observed in a more physiologically relevant setting. To test this, we
182 cultured *V. cholerae* strains with CBP intact, a P_{chb}-mCherry reporter, and a
183 construct that constitutively expresses GFP (P_{const2}-GFP) on chitin beads (**Fig.**

184 **2A**). The P_{const2}-GFP construct (derived from the insulated *proD* promoter (22))
185 served as an internal control for noise in gene expression and was used to
186 normalize P_{chb}-mCherry expression in single cells (see Methods for details).
187
188 When cells were cultured on chitin beads, both the parent strain and the Δ*hapR*
189 strain exhibited a bimodal distribution of P_{chb} expression (**Fig. 2A-C**). There were
190 at least two possible explanations for the observed bimodality in P_{chb} gene
191 expression in this experiment. One, the signaling pathway that leads to activation
192 of *chb* has switch-like behavior that results in a population that exhibits bimodality
193 in *chb* expression. Or two, the environment during growth on chitin beads is
194 heterogeneous and only some cells within the population have access to the
195 chitin oligosaccharides necessary for activation of *chb*. Those cells that do not
196 have access to chitin do not activate P_{chb} expression (P_{chb} Off), while those that
197 do have access to chitin do induce P_{chb} expression (P_{chb} On). To differentiate
198 between these two possibilities, we induced expression of P_{chb} either using the
199 native inducer, chitin oligosaccharides, or genetically by deleting *cbp*. If the
200 signaling circuit responsible for P_{chb} activation has switch-like behavior, we would
201 predict that bimodality in gene expression would be maintained in both of these
202 conditions; however, if bimodality is the result of heterogeneous access to chitin
203 oligosaccharides when cells are cultured on chitin beads, we would expect
204 bimodality to be lost. When P_{chb} was induced by chitin oligosaccharides or *via*
205 deletion of *cbp*, all cells in the population are uniformly "P_{chb} On" (**Fig. 2D, 2F**)
206 and the population becomes unimodal (**Fig. 2E, 2G**). Thus, these results showed
207 that only the "P_{chb} On" cells have access to chitin oligosaccharides when grown
208 on chitin beads. These results are consistent with chitin-induction of natural
209 transformation on chitin beads, where cells display bimodality in gene expression
210 that is also likely due to heterogeneous access to inducing chitin
211 oligosaccharides (23).
212
213 Next, we tested whether HapR influenced activation of P_{chb} on chitin beads by
214 just assessing the expression level among "P_{chb} On" cells. As observed in bulk
215 populations, the Δ*hapR* strain exhibited a ~1.7 fold increase in P_{chb} expression
216 when cultured on chitin beads (**Fig. 2C**) and a ~2.5 fold increase when cultured
217 with chitin oligosaccharides (**Fig. 2E**). These values were consistent with the ~2-
218 fold increase in P_{chb} expression observed in single cells when the population was
219 induced via deletion of *cbp* (**Fig. 2G**). Finally, native *chb* transcripts (measured
220 *via* qRT-PCR) were also induced ~2-fold higher in a Δ*hapR* mutant compared to
221 the parent when strains were induced with chitin oligosaccharides (**Fig. S2**).
222 Together, these results indicate that HapR is a *bona fide* repressor of P_{chb} under
223 physiologically relevant inducing conditions.
224
225 *HapR repression of P_{chb} is conserved in other V. cholerae El Tor isolates*
226 Previously, it was suggested that HapR was an activator of P_{chb} expression in the
227 *V. cholerae* El Tor isolate A1552 (16). Specifically, the authors showed that
228 deletion of *hapR* resulted in a decrease in P_{chb} expression when cells were
229 cultured on chitin flakes. In the present study, we use the *V. cholerae* El Tor

230 isolate E7946 to study P_{chb} regulation. To assess if HapR exhibits different
231 effects on P_{chb} expression depending on the strain background, we assessed
232 expression of a P_{chb}-mCherry reporter in *hapR*$^+$ and Δ*hapR* derivatives of both
233 E7946 and A1552. Consistent with our previous results, we observed that P_{chb}
234 expression is elevated ~2-fold in the Δ*hapR* derivative of both strain backgrounds
235 when induced with chitin oligosaccharides or via deletion of *cbp*, which is
236 consistent with HapR acting as a repressor of this locus (**Fig. S3**). It is unclear
237 what explains the discrepancy between our findings and those that were
238 previously reported; however, these data suggest that they cannot be attributed
239 to differences between strain backgrounds.
240
241 *Deletion of HapR does not confer a growth advantage during growth on*
242 *chitobiose*
243 Our data indicates that in the absence of HapR, P_{chb} expression is elevated. The
244 *chb* locus encodes the genes required for uptake and degradation of the chitin
245 disaccharide, chitobiose. Thus, we wanted to assess if the increased expression
246 of P_{chb} confers a fitness advantage to Δ*hapR* cells during growth on chitobiose.
247 To test this, we conducted competitive growth assays with a 1:1 mixture of a
248 parent and a Δ*hapR* mutant strain on minimal medium with chitobiose as the sole
249 carbon source. We hypothesized that if the Δ*hapR* mutant had a competitive
250 growth advantage due to increased expression of *chb*, then it should outcompete
251 the parent strain in this assay. Even after ~48 generations of growth on
252 chitobiose, however, we did not observe a competitive advantage for the Δ*hapR*
253 mutant (**Fig. S4**). HapR is a global regulator that controls the expression of
254 dozens of genes (24). Thus, even though a Δ*hapR* mutant has increased P_{chb}
255 expression, there may be negative pleiotropic effects associated with the Δ*hapR*
256 mutation that masks any competitive advantage of derepression of P_{chb} in this
257 mutant during growth on chitobiose.
258
259 *HapR binds P_{chb} in vitro and in vivo*
260 Thus far, our data suggest that HapR is a repressor of P_{chb}, but it does not
261 distinguish whether HapR is a direct or indirect regulator of this locus. To assess
262 if HapR could be regulating P_{chb} directly, we used an *in silico* approach to identify
263 putative HapR binding sites in P_{chb} based on consensus binding sequences
264 generated for the HapR homologs LuxR (from *Vibrio harveyi*) and SmcR (from *V.*
265 *vulnificus*) via chromatin immunoprecipitation sequencing (ChIP-seq) (25, 26).
266 Using the Motif Alignment and Search Tool (MAST) in the Multiple Em for Motif
267 Elicitiation (MEME) Suite (27), we identified two potential HapR binding sites in
268 P_{chb} (**Fig. 3A**). Interestingly, these binding sites (BSs) overlap with other elements
269 in the *chb* promoter required for transcriptional activation. HapR BS 1 overlaps
270 with the SlmA binding site, which is a critical activator of P_{chb} expression (11).
271 HapR BS 2 overlaps with the -35 signal, which is required for RNA polymerase to
272 bind to the promoter and initiate transcription. This sequence analysis suggests
273 that the repressive effect of HapR may be due to HapR binding directly
274 antagonizing SlmA and/or RNAP at this locus.
275

276 We next sought to determine whether HapR could directly bind to P_{chb} using both
277 *in vitro* and *in vivo* approaches. First, we tested whether HapR could bind to P_{chb}
278 *in vitro* using EMSA assays. Consistent with the presence of two HapR binding
279 sites in P_{chb}, we observed two shifts by EMSA when using a DNA probe of the
280 *chb* promoter (**Fig. 3B**). HapR does not regulate the ClpP promoter and thus did
281 not bind P_{clpP} (**Fig. 3B**), which is consistent with previous studies (28). EMSAs
282 were also done using 32 bp probes that encompassed each putative HapR BS
283 (probe sequences in **Fig. 3A**). We observed that HapR was able to bind to both
284 probes, suggesting that HapR binds to both HapR BS 1 and HapR BS 2 (**Fig.**
285 **3C**). Next, we wanted to assess if HapR bound to P_{chb} *in vivo via* ChIP assays
286 under physiologically relevant conditions. To that end, we first generated a
287 FLAG-HapR strain that was functional for regulating P_{chb} expression (**Fig. S5**).
288 Using this strain in ChIP-qPCR assays, we found that P_{chb} was, indeed, bound by
289 HapR *in vivo*, while the negative control P_{clpP} locus was not bound by HapR (**Fig.**
290 **3D**). Together, these data demonstrate that HapR binds to P_{chb}, which suggests
291 that it is a direct repressor of this locus.
292
293 *Quorum sensing regulates expression of P_{chb} through the cholera-specific*
294 *autoinducer CAI-1*
295 HapR is the master regulator of quorum sensing (QS) in *V. cholerae*, and is
296 highly expressed at high cell density (HCD) (29). Thus far, we have established
297 that HapR is a repressor of P_{chb} expression. Next, we wanted to probe the role of
298 QS in regulating P_{chb}. To that end, we sought to test the effect of mutations in
299 genes upstream of HapR in the *V. cholerae* QS cascade on P_{chb} induction and
300 HapR protein levels.
301
302 QS in *Vibrio* species is controlled by autoinducer-responsive sensor proteins that
303 indirectly modulate phosphorylation of the response regulator LuxO, which in turn
304 indirectly regulates production of HapR (14). When autoinducer concentrations
305 are low (*i.e.*, at low cell density (LCD)), multiple histidine kinase sensors acts as
306 kinases (30-32). This results in high levels of phosphorylated LuxO, which
307 prevents HapR production (**Fig. S6A**) (33). By contrast, at high autoinducer
308 concentrations (*i.e.*, at HCD), the sensors act as phosphatases, which ultimately
309 leads to dephosphorylation of LuxO and allows for HapR production (**Fig. S6B**)
310 (14, 34).
311
312 First, we assessed the impact of HCD on P_{chb} induction and HapR levels by
313 deleting *luxO*, which genetically locks cells in a HCD state. Induction of the
314 parent strain is tested under HCD conditions, thus, as expected, HapR levels
315 were similar between the parent and the Δ*luxO* mutant; accordingly, expression
316 of P_{chb} was also similar between the parent and Δ*luxO* (**Fig. 4**). Next, we tested
317 the effect of LCD on P_{chb} and HapR expression by generating a $luxO^{D47E}$ mutant,
318 which mimics phosphorylated LuxO and genetically locks cells in a LCD state. In
319 this strain, we saw that P_{chb} expression increased and was correlated with a
320 decrease in HapR protein levels (**Fig. 4**). Together, these data suggest that
321 HapR repression of P_{chb} is mediated through the canonical QS circuit.

322
323 Next, we wanted to move further upstream in the QS regulatory cascade to
324 address if distinct autoinducers differentially affected expression of P_{chb} and
325 HapR. There are four parallel histidine kinase sensors that coordinate QS-
326 dependent control of HapR expression (13); however, the autoinducer signal is
327 only known for two of these systems. The sensor LuxPQ is responsive to the
328 inter-species autoinducer AI-2, and the sensor CqsS is responsive to the *V.*
329 *cholerae*-specific autoinducer CAI-1 (**Fig. S6**) (35). To assess the role of each
330 autoinducer in regulation of P_{chb}, we made mutations to the synthase genes
331 responsible for production of each autoinducer. LuxS makes AI-2 (36) and CqsA
332 makes CAI-1 (35) (**Fig. S6**). In a strain that no longer produces AI-2 (Δ*luxS*),
333 expression of P_{chb} was similar to that observed in the parent and HapR levels
334 remained similar in these two strains (**Fig. 4**). By contrast, a strain that is unable
335 to produce CAI-1 (Δ*cqsA*) had increased expression of P_{chb}, likely due to the low
336 level of HapR produced (**Fig. 4**). The observed decrease in P_{chb} expression in the
337 Δ*cqsA* background was, indeed, due to a lack of CAI-1 production as
338 exogenously adding back synthetic CAI-1 restored HapR levels and repression of
339 P_{chb} to the parent level (**Fig. 4**). In addition, a strain that does not make CAI-1
340 induced P_{chb} to the same level as a strain that does not produce both CAI-1 or
341 HapR (**Fig. 4**). This epistasis indicates that CAI-1 production and HapR are
342 involved in the same regulatory pathway for modulating expression of P_{chb}.
343 These data support previous results, which indicate that CqsS signaling plays a
344 dominant role in regulating HapR (23, 35, 37, 38). Together, these results
345 indicate that P_{chb} expression is strongly influenced by QS signaling mediated by
346 the *V. cholerae*-specific autoinducer CAI-1 and less via the inter-species
347 autoinducer AI-2.
348
349 **Discussion**
350 Here, we show that HapR acts as a repressor of chitobiose utilization genes in *V.*
351 *cholerae*. When this organism forms communities on a chitinous surface, chitin
352 induces expression of P_{chb} through activation of the chitin sensor ChiS (**Fig. 5**).
353 *V. cholerae* then modulates P_{chb} expression depending on the presence of other
354 *V. cholerae* cells, which it senses via the *V. cholerae*-specific autoinducer CAI-1.
355 At low CAI-1 concentrations, P_{chb} expression is high because the repressor HapR
356 is produced at a low level (**Fig. 5A**). At high CAI-1 concentrations, HapR is
357 produced at higher levels and can repress P_{chb} expression (**Fig. 5B**). As the
358 HapR binding sites in P_{chb} overlap with the SlmA binding site and the -35 signal,
359 it is possible that HapR competes with these activators for binding at P_{chb}. Thus,
360 HapR-mediated repression may occur through antagonism of the binding activity
361 of SlmA and/or RNAP at P_{chb}.
362
363 When HapR is produced, it gets proteolyzed by the ClpAP machine (**Fig. 5B**).
364 While the dynamic range of HapR-dependent P_{chb} repression is only ~2-fold
365 when ClpAP is intact, the dynamic range of repression increases to ~7-fold in the
366 absence of ClpAP. Thus, it is tempting to speculate that regulation of ClpAP may
367 modulate P_{chb} expression under some conditions. Currently, however, little is

368 known about the regulation of ClpAP in *V. cholerae*. ClpAP is induced during
369 heat shock in *V. vulnificus* (21). Also, in *E. coli*, ClpP expression is induced
370 during heat shock (39-41). Thus, it is believed that the ClpP protease plays a role
371 in the heat shock response. In *Bacillus subtilis*, ClpP is upregulated under
372 various stress conditions, suggesting that this protease may also be induced by a
373 general stress response (42). Thus, one possibility is that stress-dependent
374 regulation of ClpAP indirectly regulates P_{chb}. It has also been hypothesized that
375 *V. cholerae* makes use of proteolysis machines to rapidly respond to changes in
376 their environment; namely, the transition from the human gut to the aquatic
377 environment after infection (43). ClpAP acting as an activator of P_{chb} may be a
378 way for cells to rapidly induce expression of a locus that is not important in the
379 human gut, but is useful for survival in its aquatic reservoir. Consistent with this
380 idea, *chb* is induced late in infection, suggesting this is a critical locus for
381 preparing to re-enter the aquatic environment after infection of a host (44).
382
383 The mechanisms underlying distinct responses to AI-2 or CAI-1 remain a topic of
384 interest in QS. It has been shown that the CAI-1 sensor CqsS plays a dominant
385 role over LuxPQ in modulating HapR levels. Thus, it remains possible that the
386 presence of CAI-1 allows for more robust regulation of HapR-regulated genes.
387 CAI-1 has been shown to be critical for expression of the virulence factor *hapA*
388 (38), natural transformation (15), and for repressing chitobiose utilization as
389 shown in this study. HapA is a protease that has been implicated in mediating *V.*
390 *cholerae* detachment from host epithelial cells, thereby promoting dissemination
391 of cells back into the aquatic environment (45, 46); natural transformation and
392 chitin utilization aid in *V. cholerae* fitness in the marine environment. By contrast,
393 expression of *tcpA*, a protein which contributes to *V. cholerae* pathogenesis in
394 the human gut, was shown to be primarily regulated by AI-2 (37). It is tempting to
395 speculate that CAI-1 controls *V. cholerae* behaviors important for marine survival,
396 whereas AI-2 controls behaviors involved in infection. It has been hypothesized
397 that sensing both of these autoinducers plays a critical role in biofilm dispersal,
398 and that only when both are sensed, *V. cholerae* cells are induced to leave a
399 surface (*i.e.* QS works as a coincidence detector for both signals) (37). Thus,
400 signaling *via* distinct autoinducers may allow *V. cholerae* to modulate responses
401 depending on the context of the environment they inhabit.
402
403 The data we present here suggests that at HCD, *V. cholerae* dampens its
404 expression of a chitin utilization locus. Below, we speculate on a few reasons
405 why this regulation may be advantageous. Chitin polymers in the shells of
406 crustacean zooplankton are long chain polysaccharides in a crystalline insoluble
407 lattice. In order to be used as a nutrient source, the long chain chitin must be
408 broken down into smaller, soluble chitin oligosaccharides. *V. cholerae* secretes
409 chitinases that enzymatically degrade insoluble chitin into soluble chitin
410 oligosaccharides for uptake and catabolism. The production and secretion of
411 chitinases is an energetically costly process; thus, liberated chitin is a valuable
412 “public good” in the context of a chitin biofilm (47). So, it is possible that QS
413 regulation of chitin utilization allows *V. cholerae* to modulate chitin uptake based

414 on the composition of its microbial community. When the level of *V. cholerae*
415 cells (and the corresponding concentration of cholera specific autoinducer CAI-1)
416 in the community is high, chitin uptake may decrease among individual cells
417 within the population in an effort to "share" liberated chitin oligosaccharides. By
418 contrast, when the level of *V. cholerae* in the community is low, sensing of only
419 the inter-species signal AI-2 (which is produced by many bacterial species) does
420 not suppress chitin uptake and utilization, thus, allowing the *V. cholerae* within
421 this population to maximally compete for liberated chitin oligosaccharides.
422
423 Another possibility is that this regulation allows *V. cholerae* to control its
424 production of toxic metabolites. In a previous study, it was shown that cells in a
425 HCD state alter their metabolic flux to produce neutral byproducts as opposed to
426 organic acids when grown in LB supplemented with a fermentable sugar like
427 glucose (48). This regulation allows for a more stable community; by contrast,
428 cells locked in a LCD state will excrete harmful metabolic byproducts, which
429 leads to the demise of the community (48). It has been shown that *V. cholerae*
430 excretes ammonium as a potentially toxic byproduct when grown on chitin (16).
431 Also, because chitin oligosaccharides likely feed into glycolysis, it is possible that
432 catabolism of chitin results in the production of potentially toxic organic acids.
433 Thus, repressing chitin uptake and utilization may also help slow the rate of
434 metabolism to prevent the accumulation of toxic intermediates in a dense
435 community setting.
436
437 **Materials & Methods**
438 *Bacterial strains and culture conditions*
439 *V. cholerae* strains were routinely grown at 30°C in LB medium and on LB agar
440 supplemented when necessary with carbenicillin (20 µg/mL or 50 µg/mL),
441 kanamycin (50 µg/mL), spectinomycin (200 µg/mL), trimethoprim (10 µg/mL),
442 and/or chloramphenicol (2 µg/mL). Strains were grown in DASW medium for
443 microscopy (see below for details), Instant Ocean for generating mutant strains
444 (see below for details), or M9 minimal medium for competition experiments (see
445 below for details).
446
447 *Transposon mutagenesis*
448 Transposon mutant libraries were generated with a $Carb^R$ mini-Tn10 transposon
449 exactly as previously described (49). Briefly, the transposon mutagenesis
450 plasmid pDL1086 was first mated into parent strains containing chromosomally-
451 integrated P_{chb}-*lacZ* and a Δ*cbp* mutation (activator screen) or Δ*clpA* Δ*cbp*
452 mutations (Δ*clpA* counter-screen). The parent strains also carried a
453 chromosomally-integrated P_{chb}-mCherry reporter at an ectopic site to ensure that
454 candidate transposon mutants affected expression of P_{chb} and did not simply
455 disrupt the P_{chb}-*lacZ* reporter. The activator screen parent also carried an
456 additional copy of ChiS at an ectopic site, which prevented transposon hits in this
457 known regulator of P_{chb}. Transposition was induced by plating cultures on LB
458 agar supplemented with 50 µg/mL Carb at 42°C. To screen colonies, plates also

459 contained 40 µg/mL X-gal and 5 mM IPTG. IPTG was added to competitively
460 inhibit the basal activity of the P_{chb}-*lacZ* reporter.
461
462 The sequence of transposon-genomic junctions in transposon mutants were
463 determined by inverse PCR followed by Sanger sequencing. Briefly, genomic
464 DNA was purified from mutants of interest and digested with the FatI restriction
465 enzyme per manufacturer's instructions (NEB). Digested genomic DNAs were
466 then incubated with T4 DNA ligase per manufacturer's instructions (NEB) to
467 generate self-ligated circles. The transposon-genomic junction was then
468 amplified by PCR using the primers specified in **Table 2** and subsequently
469 Sanger sequenced (Eurofins Genomics).
470
471 *Generating mutant strains*
472 *V. cholerae* E7946 served as the parent for all strains generated in this study,
473 except for those used in **Fig. S3** where we compare E7946 to A1552 (50, 51).
474 Mutant constructs were generated by splicing-by-overlap extension (SOE) PCR
475 exactly as previously described with the primers indicated in **Table 2**. (52). PCRs
476 were performed to generate Up (F1/R1), Middle, and Down (F2/R2) arms. Up
477 and Down arms were designed to have 3kb arms of homology to the genome at
478 the site targeted for mutagenesis. All three arms were then mixed and used as
479 template for SOE PCR reactions with the F1 and R2 primers to generate the full
480 length mutant construct SOE product. Mutant constructs were introduced into *V.*
481 *cholerae* cells by chitin-induced natural transformation and/or cotransformation
482 exactly as previously described (53, 54) or by chitin-independent transformations
483 using a plasmid that ectopically expresses *tfoX* and *qstR* as previously described
484 (55). For chitin-dependent natural transformation, *V. cholerae* was grown to mid-
485 log in LB medium, washed with instant ocean medium (7 g/L; Aquarium
486 Systems), and incubated with chitin flakes (Alfa Aesar) at final OD_{600} of 0.1
487 overnight at 30°C. The next day, SOE PCR products were added to chitin
488 induced cells, incubated at 30°C for 5 hrs, and then outgrown and plated on
489 selective media. For chitin-independent transformation, cells harboring
490 pMMB67EH-*tfoX*-*qstR* were grown overnight in LB medium supplemented with
491 100 µM IPTG and 1 µg/mL chloramphenicol. The next day, 7 µL of the overnight
492 culture was diluted into 350 µL of instant ocean medium. Then, SOE products
493 were added as described above for chitin-dependent transformations. Mutant
494 strains were confirmed by colony PCR, MAMA PCR (56), and/or sequencing. A
495 complete list of strains and primers used in this study are outlined in **Table 1** and
496 **Table 2**, respectively.
497
498 *Measuring GFP and mCherry fluorescence in bulk populations*
499 GFP and mCherry fluorescence in reporter strains was determined exactly as
500 previously described (57). Briefly, single colonies were grown in LB overnight at
501 30°C. Where indicated, media was supplemented with 10 µM CAI-1. CAI-1 was
502 synthesized exactly as previously described (58). The next day, cells were
503 washed and resuspended to an OD_{600} of 1.0 in instant ocean medium (7 g/L;

504 Aquarium systems). Fluorescence was determined on a BioTek H1M plate
505 reader. For GFP measurements, excitation was set to 500 nm and emission was
506 set to 540 nm; for mCherry measurements, excitation was set to 580 nm and
507 emission was set to 610 nm.
508
509 *Antibody generation*
510 Purified *Vibrio harveyi* LuxR protein (300 µg; purified as previously described
511 (59)) was sent to Cocalico Biologicals Inc. for serial injection into a rabbit host for
512 antibody generation. Serum obtained from the third bleed has been used for
513 Western analyses.
514
515 *Western blotting*
516 From overnight cultures, cells were concentrated to an OD_{600} of 20 in instant
517 ocean medium. Cells were lysed on a FastPrep-24 Classic Instrument at 4°C,
518 then lysates were clarified by centrifugation. Lysates were then boiled with an
519 equal volume of 2x SDS PAGE sample buffer (220 mM Tris pH 6.8, 25%
520 glycerol, 1.2% SDS, 0.02% Bromophenol Blue, and 5% β-mercaptoethanol).
521 Proteins were separated on a 15% SDS polyacrylamide gel by SDS
522 electrophoresis, electropheretically transferred to a PVDF membrane, and
523 probed with rabbit polyconal α-LuxR serum or mouse monoclonal α-RpoA
524 (Biolegend) primary antibodies. LuxR is the HapR homolog in *Vibrio harveyi* and
525 has 72% identity and 86% similarity to *V. cholerae* HapR. The LuxR antibody
526 was empirically found to be cross-reactive with *V. cholerae* HapR, and so it was
527 used to detect HapR protein levels. Blots were then incubated with α-rabbit or α-
528 mouse HRP conjugated secondary antibodies, developed using Pierce ECL
529 Western Blotting Substrate (ThermoFisher), and exposed to film.
530
531 *Chitin bead culturing*
532 Chitin beads (200 µL of a 50% slurry; NEB) and overnight cultures of the
533 indicated strains were washed with defined artificial salt water medium (DASW),
534 which was prepared exactly as previously described (8). Chitin beads were
535 inoculated with *V. cholerae* cells to an OD_{600} of 0.1 in a final volume of 5 mL in a
536 Costar 6-well plate (Corning). Chitin mixtures were incubated statically at 30°C
537 for 7 days before imaging.
538
539 *Microscopy data collection and analysis*
540 To image chitin beads, cultured beads were gently transferred to a coverslip
541 using wide-bore pipette tips. To image chitin grown cells, chitin bead reactions
542 were vortexed then centrifuged at 250 x g for 1 minute. Cells found in the
543 supernatant were transferred to a coverslip. To image Δ*cbp* strains, overnight
544 cultures grown in LB were washed and resuspended to an OD_{600} of 0.2 in DASW
545 and then transferred to a coverslip. Samples on the coverslip were placed under
546 a 0.2% gelzan pad and imaged on an inverted Nikon Ti-2 microscope with a Plan
547 Apo 60x objective, YFP & mCherry filter cubes, a Hamamatsu ORCAFlash 4.0
548 camera, and Nikon NIS Elements imaging software.
549

550 The strains used to examine P_{chb} expression across a population contained 1) a
551 P_{chb}-mCherry reporter and 2) a reporter that drove constitutive expression of
552 GFP, P_{const2}-GFP. By using these reporters, the expression of the P_{chb}-mCherry
553 could be normalized to GFP expression in each cell. Images were analyzed on
554 Fiji using the MicrobeJ plugin (60) to determine mean intensity of cells in the YFP
555 and mCherry channels. GFP was assessed using a YFP filter set to avoid
556 background fluorescence from chitin beads, which was stronger in the GFP
557 channel. Background fluorescence was subtracted from each channel and the
558 mCherry / GFP fluorescence was determined for each individual cell.
559
560 *HapR protein purification*
561 A plasmid expressing a hexahistidine-tagged *hapR* wild-type allele was
562 generated using Gibson assembly. The *hapR* insert was amplified from *V.*
563 *cholerae* E7946 and inserted into a pET28b vector (Novagen) using the primers
564 listed in **Table 2**. The plasmid was then electroporated into *E. coli* BL21(DE3) for
565 protein overexpression. This strain was grown overnight in LB medium with
566 kanamycin, back-diluted 1:100 into 1 L of LB medium with kanamycin, and grown
567 to an OD_{600} of 0.4-0.6 at 30°C. Expression of HapR was induced by IPTG to a
568 final concentration of 1 mM and cultures grown for 4 h shaking at 30°C. The cells
569 were pelleted and frozen at -80°C. The pellet was resuspended in 25 mL Buffer A
570 (25 mM Tris pH 8, 500 mM NaCl), and an Avestin EmulfiFlex-C3 emulsifier was
571 used to lyse cells. The soluble lysate was applied to a HisTrap HP Ni-NTA
572 column using an Äkta Pure FPLC in Buffer A and eluted from the column with a
573 gradient of Buffer B (25 mM Tris pH 8, 500 mM NaCl, 1 M imidazole). The
574 purified protein was concentrated to approximately 5 ml using Sartorius Vivaspin
575 Turbo 10,000 MWCO centrifugal concentrators. The sample was manually
576 injected into the Äkta Pure and separated via size exclusion chromatography on
577 a HiLoad™ 16/600 Superdex™ 75 pg column equilibrated with gel filtration buffer
578 (25 mM Tris pH 7.5, 200 mM NaCl). Eluted fractions were analyzed by SDS-
579 PAGE (15% gel), pooled, and concentrated using the same centrifugal
580 concentrators previously mentioned. The samples were then immediately frozen
581 in liquid nitrogen with a final concentration of 10% glycerol and stored at -80°C.
582
583 *Electrophoretic mobility shift assay (EMSA)*
584 Binding reactions contained 10 mM Tris HCl pH 7.5, 1 mM EDTA, 10 mM KCl, 1
585 mM DTT, 50 µg/mL BSA, 0.1 mg/mL salmon sperm DNA, 5% glycerol, 1 nM of a
586 Cy5 labeled DNA probe, and HapR at the indicated concentrations (diluted in 10
587 mM Tris pH 7.5, 10 mM KCl, 1 mM DTT, and 5% glycerol). Reactions were
588 incubated at room temperature for 20 minutes in the dark, then
589 electrophoretically separated on polyacrylamide gels in 0.5x Tris Borate EDTA
590 (TBE) buffer. Gels were imaged for Cy5 fluorescence on a Typhoon-9210
591 instrument. Short DNA probes (30bp) were made by end-labeling one primer of a
592 complementary pair (primers listed in **Table 2**) using 20 µM Cy5-dCTP and
593 Terminal deoxynucleotidyl Transferase (TdT; Promega). Complementary primers
594 (one labeled with Cy5 and the other unlabeled) were annealed by slow cooling at
595 equimolar concentrations in annealing buffer (10 mM Tris pH 7.5 and 50 mM

596 NaCl). P_{chb} and P_{clpP} probes were made by Phusion PCR, where Cy5-dCTP was
597 included in the reaction at a level that would result in incorporation of 1–2 Cy5
598 labeled nucleotides in the final probe as previously described.
599
600 *ChIP-qPCR assays*
601 Assays were carried out exactly as previously described (10). Briefly, overnight
602 cultures were diluted to an OD_{600} of 0.08 and then grown for 6 hours at 30°C.
603 Cultures were crosslinked using 1% paraformaldehyde, then quenched with a 1.2
604 molar excess of Tris. Cells were washed with PBS and stored at -80°C overnight.
605 The next day, cells were resuspended in lysis buffer (1x FastBreak cell lysis
606 reagent (Promega), 50 µg/mL lysozyme, 1% Triton X-100, 1 mM PMSF, and 1x
607 protease inhibitor cocktail; 100x inhibitor cocktail contained the following: 0.07
608 mg/mL phosphoramidon (Santa Cruz), 0.006 mg/mL bestatin
609 (MPbiomedicals/Fisher Scientific), 1.67 mg/mL AEBSF (DOT Scientific), 0.07
610 mg/mL pepstatin A (Gold Bio), 0.07 mg/mL E64 (Gold Bio)) and then lysed by
611 sonication, resulting in a DNA shear size of ~500 bp. Lysates were incubated
612 with Anti-FLAG M2 Magnetic Beads (Sigma), washed to remove unbound
613 proteins, and then bound protein-DNA complexes were eluted off with SDS.
614 Samples were digested with Proteinase K, then crosslinks were reversed. DNA
615 samples were cleaned up and used as template for quantitative PCR (qPCR)
616 using iTaq Universal SYBR Green Supermix (Bio-Rad) and primers specific for
617 the genes indicated (primers are listed in **Table 2**) on a Step-One qPCR system.
618 Standard curves of genomic DNA were included in each experiment and were
619 used to determine the abundance of each amplicon in the input (derived from the
620 lysate prior to ChIP) and output (derived from the samples after ChIP). Primers to
621 amplify *rpoB* served as a baseline control in this assay because HapR does not
622 bind this locus. Data are reported as 'Fold Enrichment', which is defined as the
623 ratio of the test promoter (P_{chb} or P_{clpP}) / *rpoB* found in the output divided by the
624 same ratio found in the input.
625
626 *Chitobiose competition*
627 Overnight cultures grown in LB were washed with M9 medium and mixed 1:1.
628 For each growth reaction, 10^2 cells of this mixture was added to M9 medium
629 supplemented with 0.2% chitobiose and 10 µM synthetic CAI-1 and grown
630 shaking at 30°C for 24 hours. After 24 hours, ~10^2 cells from this mixture was
631 used to inoculate fresh growth reactions to achieve additional generations of
632 growth on chitobiose. This was repeated a third time after another 24 hours. CAI-
633 1 was supplemented throughout these experiments to ensure consistently high
634 levels of HapR expression throughout transfer steps. After each 24 hour growth
635 period, the CFU/mL was determined for each strain in the mixture by dilution
636 plating on LB agar supplemented with X-gal. Competing strains were discerned
637 by blue/white screening as one strain was *lacZ*$^+$ and the other was Δ*lacZ*. A *lacZ*$^+$
638 strain was competed against a Δ*lacZ* strain (parent : parent competition) or
639 against a Δ*lacZ* Δ*hapR* strain (Δ*hapR* : parent competition). *V. cholerae* can grow
640 on chitobiose through the activity of two sugar transporters: the GlcNAc PTS
641 transporter (VC0995) or the chitobiose ABC transporter (VC0616-0620).

642 Because we wanted to study the regulation of the transporter encoded within the
643 *chb* locus, all strains for this assay had a deletion in VC0995, which renders
644 growth on chitobiose dependent on the *chb* locus as previously described (11).
645 Competitive indices were calculated as the CFU ratio of Δ*lacZ* / *lacZ*$^+$ after
646 growth for the indicated number of generations divided by the CFU ratio of the
647 Δ*lacZ* / *lacZ*+ in the initial inoculum.
648
649 *Statistics*
650 Statistical comparisons were determined using Student's t-test or One-way
651 ANOVA with Tukey's post-test using GraphPad Prism software.
652
653 **Acknowledgements**
654 We thank Ryan Chaparian for offering experimental advice, David Grainger for
655 helpful discussions, and Wai-Leung Ng for providing synthetic CAI-1. This work
656 was supported by grant R35GM128674 from the National Institutes of Health to
657 ABD and R35GM124698 from the National Institutes of Health to JVK.
658
659

660 **References**
661

662 1. Pruzzo C, Vezzulli L, & Colwell RR (2008) Global impact of *Vibrio*
663 *cholerae* interactions with chitin. *Environ Microbiol* 10(6):1400-1410.
664 2. Huq A*, et al.* (1983) Ecological relationships between *Vibrio cholerae* and
665 planktonic crustacean copepods. *Appl Environ Microbiol* 45(1):275-283.
666 3. Nahar S*, et al.* (2011) Role of Shrimp Chitin in the Ecology of Toxigenic
667 *Vibrio cholerae* and Cholera Transmission. *Front Microbiol* 2:260.
668 4. Hunt DE, Gevers D, Vahora NM, & Polz MF (2008) Conservation of the
669 chitin utilization pathway in the *Vibrionaceae*. *Appl Environ Microbiol*
670 74(1):44-51.
671 5. Colwell RR*, et al.* (2003) Reduction of cholera in Bangladeshi villages by
672 simple filtration. *Proc Natl Acad Sci U S A* 100(3):1051-1055.
673 6. Huq A*, et al.* (2010) Simple sari cloth filtration of water is sustainable and
674 continues to protect villagers from cholera in Matlab, Bangladesh. *mBio*
675 1(1).
676 7. Meibom KL*, et al.* (2004) The *Vibrio cholerae* chitin utilization program.
677 *Proc Natl Acad Sci U S A* 101(8):2524-2529.
678 8. Meibom KL, Blokesch M, Dolganov NA, Wu CY, & Schoolnik GK (2005)
679 Chitin induces natural competence in *Vibrio cholerae*. *Science*
680 310(5755):1824-1827.
681 9. Li X & Roseman S (2004) The chitinolytic cascade in *Vibrios* is regulated
682 by chitin oligosaccharides and a two-component chitin catabolic
683 sensor/kinase. *Proc Natl Acad Sci U S A* 101(2):627-631.
684 10. Klancher CA, Yamamoto S, Dalia TN, & Dalia AB (2020) ChiS is a
685 noncanonical DNA-binding hybrid sensor kinase that directly regulates the
686 chitin utilization program in *Vibrio cholerae*. *Proc Natl Acad Sci U S A* In
687 press.
688 11. Klancher CA, Hayes CA, & Dalia AB (2017) The nucleoid occlusion
689 protein SlmA is a direct transcriptional activator of chitobiose utilization in
690 *Vibrio cholerae*. *PLoS Genet* 13(7):e1006877.
691 12. Fuqua WC, Winans SC, & Greenberg EP (1994) Quorum sensing in
692 bacteria: the LuxR-LuxI family of cell density-responsive transcriptional
693 regulators. *J Bacteriol* 176(2):269-275.
694 13. Jung SA, Chapman CA, & Ng WL (2015) Quadruple quorum-sensing
695 inputs control *Vibrio cholerae* virulence and maintain system robustness.
696 *PLoS Pathog* 11(4):e1004837.
697 14. Ball AS, Chaparian RR, & van Kessel JC (2017) Quorum Sensing Gene
698 Regulation by LuxR/HapR Master Regulators in *Vibrios*. *J Bacteriol*
699 199(19).
700 15. Suckow G, Seitz P, & Blokesch M (2011) Quorum sensing contributes to
701 natural transformation of *Vibrio cholerae* in a species-specific manner. *J*
702 *Bacteriol* 193(18):4914-4924.
703 16. Sun S, Tay QX, Kjelleberg S, Rice SA, & McDougald D (2015) Quorum
704 sensing-regulated chitin metabolism provides grazing resistance to *Vibrio*
705 *cholerae* biofilms. *ISME J* 9(8):1812-1820.

17. Yamamoto S*, et al.* (2014) Regulation of natural competence by the orphan two-component system sensor kinase ChiS involves a non-canonical transmembrane regulator in *Vibrio cholerae*. *Molecular microbiology* 91(2):326-347.
18. Yamamoto S & Ohnishi M (2017) Glucose-Specific Enzyme IIA of the Phosphoenolpyruvate:Carbohydrate Phosphotransferase System Modulates Chitin Signaling Pathways in *Vibrio cholerae*. *J Bacteriol* 199(18).
19. Blokesch M (2012) Chitin colonization, chitin degradation and chitin-induced natural competence of Vibrio cholerae are subject to catabolite repression. *Environ Microbiol* 14(8):1898-1912.
20. Sauer RT & Baker TA (2011) AAA+ proteases: ATP-fueled machines of protein destruction. *Annu Rev Biochem* 80:587-612.
21. Lee KJ, Jung YC, Park SJ, & Lee KH (2018) Role of Heat Shock Proteases in Quorum-Sensing-Mediated Regulation of Biofilm Formation by *Vibrio* Species. *mBio* 9(1).
22. Davis JH, Rubin AJ, & Sauer RT (2011) Design, construction and characterization of a set of insulated bacterial promoters. *Nucleic Acids Res* 39(3):1131-1141.
23. Lo Scrudato M & Blokesch M (2012) The regulatory network of natural competence and transformation of *Vibrio cholerae*. *PLoS Genet* 8(6):e1002778.
24. Zhu J & Mekalanos JJ (2003) Quorum sensing-dependent biofilms enhance colonization in *Vibrio cholerae*. *Dev Cell* 5(4):647-656.
25. van Kessel JC, Ulrich LE, Zhulin IB, & Bassler BL (2013) Analysis of activator and repressor functions reveals the requirements for transcriptional control by LuxR, the master regulator of quorum sensing in *Vibrio harveyi*. *mBio* 4(4).
26. Lee DH*, et al.* (2008) A consensus sequence for binding of SmcR, a *Vibrio vulnificus* LuxR homologue, and genome-wide identification of the SmcR regulon. *J Biol Chem* 283(35):23610-23618.
27. Bailey TL*, et al.* (2009) MEME SUITE: tools for motif discovery and searching. *Nucleic Acids Res* 37(Web Server issue):W202-208.
28. Chaparian RR, Tran MLN, Miller Conrad LC, Rusch DB, & van Kessel JC (2020) Global H-NS counter-silencing by LuxR activates quorum sensing gene expression. *Nucleic Acids Res* 48(1):171-183.
29. Jobling MG & Holmes RK (1997) Characterization of *hapR*, a positive regulator of the *Vibrio cholerae* HA/protease gene hap, and its identification as a functional homologue of the *Vibrio harveyi* luxR gene. *Molecular microbiology* 26(5):1023-1034.
30. Freeman JA, Lilley BN, & Bassler BL (2000) A genetic analysis of the functions of LuxN: a two-component hybrid sensor kinase that regulates quorum sensing in *Vibrio harveyi*. *Molecular microbiology* 35(1):139-149.
31. Freeman JA & Bassler BL (1999) Sequence and function of LuxU: a two-component phosphorelay protein that regulates quorum sensing in *Vibrio harveyi*. *J Bacteriol* 181(3):899-906.

752 32. Neiditch MB, Federle MJ, Miller ST, Bassler BL, & Hughson FM (2005)
753 Regulation of LuxPQ receptor activity by the quorum-sensing signal
754 autoinducer-2. *Mol Cell* 18(5):507-518.
755 33. Tu KC & Bassler BL (2007) Multiple small RNAs act additively to integrate
756 sensory information and control quorum sensing in *Vibrio harveyi*. *Genes*
757 *Dev* 21(2):221-233.
758 34. Freeman JA & Bassler BL (1999) A genetic analysis of the function of
759 LuxO, a two-component response regulator involved in quorum sensing in
760 *Vibrio harveyi*. *Molecular microbiology* 31(2):665-677.
761 35. Miller MB, Skorupski K, Lenz DH, Taylor RK, & Bassler BL (2002) Parallel
762 quorum sensing systems converge to regulate virulence in *Vibrio*
763 *cholerae*. *Cell* 110(3):303-314.
764 36. Surette MG, Miller MB, & Bassler BL (1999) Quorum sensing in
765 *Escherichia coli*, *Salmonella typhimurium*, and *Vibrio harveyi*: a new family
766 of genes responsible for autoinducer production. *Proc Natl Acad Sci U S A*
767 96(4):1639-1644.
768 37. Bridges AA & Bassler BL (2019) The intragenus and interspecies quorum-
769 sensing autoinducers exert distinct control over *Vibrio cholerae* biofilm
770 formation and dispersal. *PLoS Biol* 17(11):e3000429.
771 38. Hurley A & Bassler BL (2017) Asymmetric regulation of quorum-sensing
772 receptors drives autoinducer-specific gene expression programs in *Vibrio*
773 *cholerae*. *PLoS Genet* 13(5):e1006826.
774 39. Kroh HE & Simon LD (1990) The ClpP component of Clp protease is the
775 sigma 32-dependent heat shock protein F21.5. *J Bacteriol* 172(10):6026-
776 6034.
777 40. Grossman AD, Erickson JW, & Gross CA (1984) The *htpR* gene product
778 of *E. coli* is a sigma factor for heat-shock promoters. *Cell* 38(2):383-390.
779 41. Katayama Y*, et al.* (1988) The two-component, ATP-dependent Clp
780 protease of *Escherichia coli*. Purification, cloning, and mutational analysis
781 of the ATP-binding component. *J Biol Chem* 263(29):15226-15236.
782 42. Gerth U, Kruger E, Derre I, Msadek T, & Hecker M (1998) Stress induction
783 of the *Bacillus subtilis clpP* gene encoding a homologue of the proteolytic
784 component of the Clp protease and the involvement of ClpP and ClpX in
785 stress tolerance. *Molecular microbiology* 28(4):787-802.
786 43. Pennetzdorfer N*, et al.* (2019) Regulated proteolysis in *Vibrio cholerae*
787 allowing rapid adaptation to stress conditions. *Front Cell Infect Microbiol*
788 9:214.
789 44. Schild S*, et al.* (2007) Genes induced late in infection increase fitness of
790 *Vibrio cholerae* after release into the environment. *Cell Host Microbe*
791 2(4):264-277.
792 45. Benitez JA*, et al.* (1997) Adherence of *Vibrio cholerae* to cultured
793 differentiated human intestinal cells: an in vitro colonization model. *Infect*
794 *Immun* 65(8):3474-3477.
795 46. Benitez JA, Silva AJ, & Finkelstein RA (2001) Environmental signals
796 controlling production of hemagglutinin/protease in *Vibrio cholerae*. *Infect*
797 *Immun* 69(10):6549-6553.

47. Drescher K, Nadell CD, Stone HA, Wingreen NS, & Bassler BL (2014) Solutions to the public goods dilemma in bacterial biofilms. *Curr Biol* 24(1):50-55.
48. Hawver LA, Giulietti JM, Baleja JD, & Ng WL (2016) Quorum sensing coordinates cooperative expression of pyruvate metabolism genes To maintain a sustainable environment for population stability. *mBio* 7(6).
49. McDonough E, Kamp H, & Camilli A (2016) *Vibrio cholerae* phosphatases required for the utilization of nucleotides and extracellular DNA as phosphate sources. *Molecular microbiology* 99(3):453-469.
50. Miller VL, DiRita VJ, & Mekalanos JJ (1989) Identification of *toxS*, a regulatory gene whose product enhances *toxR*-mediated activation of the cholera toxin promoter. *J Bacteriol* 171(3):1288-1293.
51. Yildiz FH, Liu XS, Heydorn A, & Schoolnik GK (2004) Molecular analysis of rugosity in a *Vibrio cholerae* O1 El Tor phase variant. *Molecular microbiology* 53(2):497-515.
52. Dalia AB, Lazinski DW, & Camilli A (2013) Characterization of undermethylated sites in *Vibrio cholerae*. *J Bacteriol* 195(10):2389-2399.
53. Dalia AB, McDonough E, & Camilli A (2014) Multiplex genome editing by natural transformation. *Proc Natl Acad Sci U S A* 111(24):8937-8942.
54. Dalia AB (2018) Natural Cotransformation and Multiplex Genome Editing by Natural Transformation (MuGENT) of *Vibrio cholerae*. *Methods Mol Biol* 1839:53-64.
55. Simpson CA, Podicheti R, Rusch DB, Dalia AB, & van Kessel JC (2019) Diversity in natural transformation frequencies and regulation across *Vibrio* species. *mBio* 10(6).
56. Cha RS, Zarbl H, Keohavong P, & Thilly WG (1992) Mismatch amplification mutation assay (MAMA): application to the *c-H-ras* gene. *PCR Methods Appl* 2(1):14-20.
57. Dalia AB (2016) RpoS is required for natural transformation of *Vibrio cholerae* through regulation of chitinases. *Environ Microbiol* 18(11):3758-3767.
58. Ng WL*, et al.* (2011) Signal production and detection specificity in *Vibrio* CqsA/CqsS quorum-sensing systems. *Molecular microbiology* 79(6):1407-1417.
59. Chaparian RR, Olney SG, Hustmyer CM, Rowe-Magnus DA, & van Kessel JC (2016) Integration host factor and LuxR synergistically bind DNA to coactivate quorum-sensing genes in *Vibrio harveyi*. *Molecular microbiology* 101(5):823-840.
60. Ducret A, Quardokus EM, & Brun YV (2016) MicrobeJ, a tool for high throughput bacterial cell detection and quantitative analysis. *Nat Microbiol* 1(7):16077.

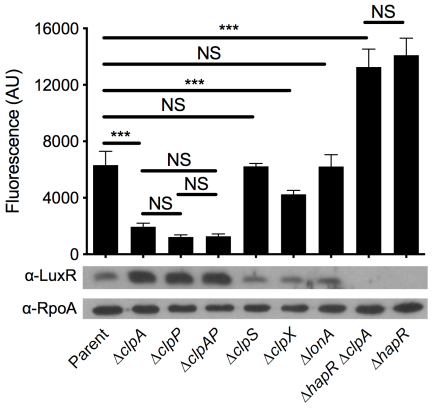

Figure 1. *HapR is a repressor of P_{chb} that is degraded by the ClpAP protease.* Expression of a P_{chb}-GFP reporter and HapR protein levels were determined in the indicated mutant strains. The parent strain contained a P_{chb}-GFP reporter and a Δ*cbp* mutation. A representative western blot is shown below bars to indicate the protein levels for HapR and RpoA (a loading control) in the corresponding strains. An antibody against LuxR, which has 72% identity and 86% similarity to HapR, is cross-reactive with HapR and so was used to detect HapR protein levels. Fluorescence of cultures was determined on a plate reader from at least six independent biological replicates and is shown as the mean ± SD. Statistical comparisons were made by one-way ANOVA with Tukey's post-test. NS, not significant. ***, $p < 0.001$.

870

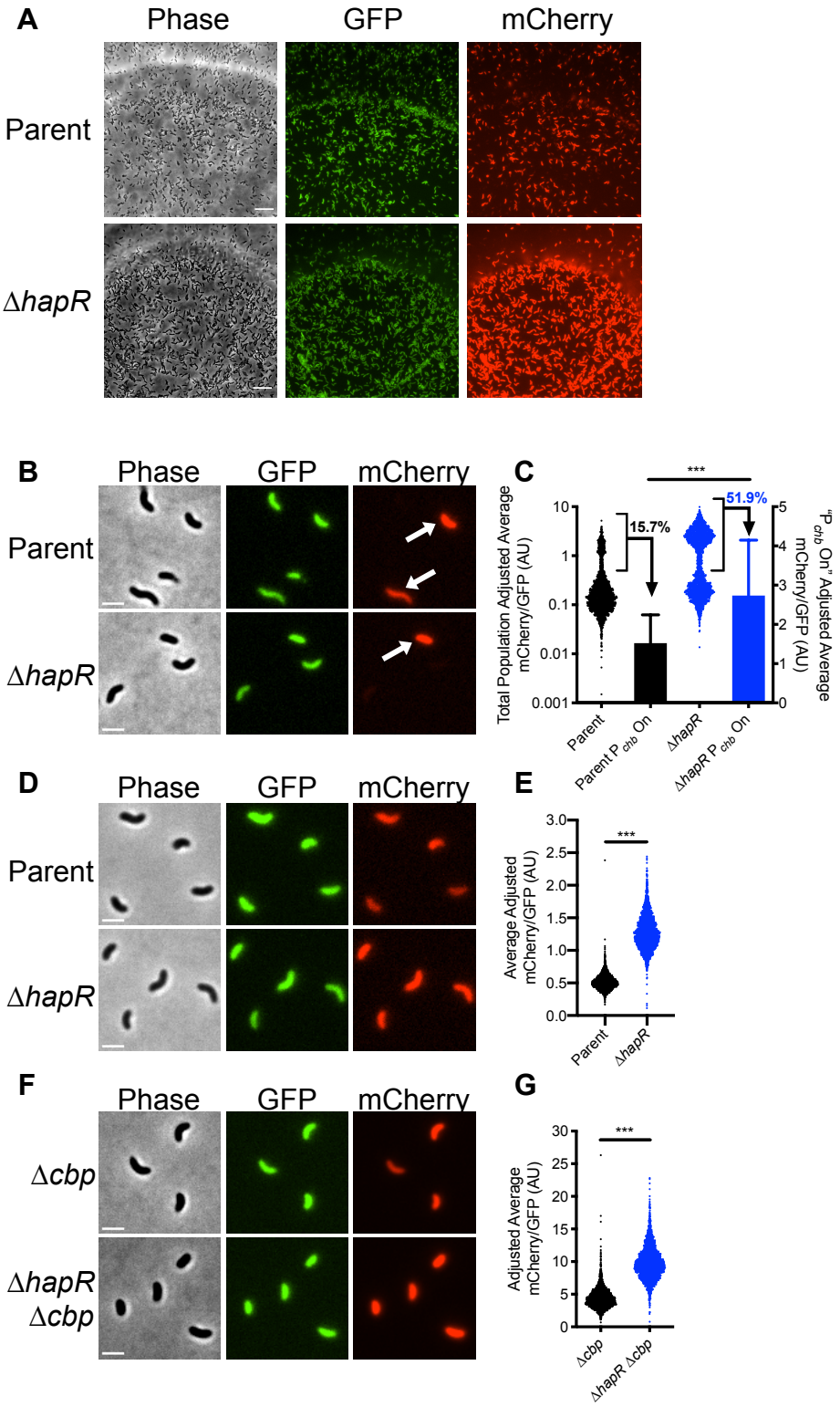

871 **Figure 2.** *HapR-mediated repression of P_{chb} occurs on chitinous surfaces.* **A**)
872 Representative images of the indicated *V. cholerae* strains grown on chitin

873 beads. The parent strain background contains both a P_{chb}-mCherry reporter and
874 a P_{const2}-GFP construct, which exhibits constitutive GFP expression. Scale bar =
875 10 µm. **B-C**) P_{chb} expression in the indicated *V. cholerae cbp*$^+$ strains grown on
876 chitin beads. **B**) Representative images of cells that were vortexed off chitin
877 beads. Arrows demarcate cells where P_{chb} expression is induced ("P_{chb} On"
878 cells). Scale bar = 2 µm. **C**) Scatter plot and bar graph showing the relative
879 expression of the P_{chb}-mCherry reporter in cells cultured on chitin beads. Scatter
880 plots (left Y-axis) represent the entire population, whereas the bars (right Y-axis)
881 represent only the "P_{chb} On" cells (bracketed in black on scatter plots). The
882 percentage of cells in the "P_{chb} On" population is indicated. n = 2120 for Parent; n
883 = 2191 for Δ*hapR;* n = 333 for Parent P_{chb} On; n = 1139 for Δ*hapR* P_{chb} On. Data
884 shown are from two independent biological replicates. **D-E**) P_{chb} expression of
885 the indicated *V. cholerae* strains where P_{chb} expression is induced by chitin
886 oligosaccharides. **D**) Representative images of cells grown with chitin
887 oligosaccharides. Scale bar = 2 µm. **E**) Scatter plot showing the relative
888 expression of a P_{chb}-mCherry reporter in the indicated *V. cholerae* strains. n =
889 2735 for Parent; n = 2384 for Δ*hapR.* Data shown are from two independent
890 biological replicates. **F-G**) P_{chb} expression of the indicated *V. cholerae* strains
891 where P_{chb} expression is induced via deletion of *cbp*. **F**) Representative images
892 of cells grown in the absence of chitin. Scale bar = 2 µm. **G**) Scatter plot showing
893 the relative expression of a P_{chb}-mCherry reporter in the indicated *V. cholerae*
894 strains. n = 2407 for Δ*cbp*; n = 2313 for Δ*hapR* Δ*cbp.* Data shown are from two
895 independent biological replicates. Statistical comparisons in **D**, **G**, and **J** were
896 made using Student's t-test. ***, $p < 0.001$.
897

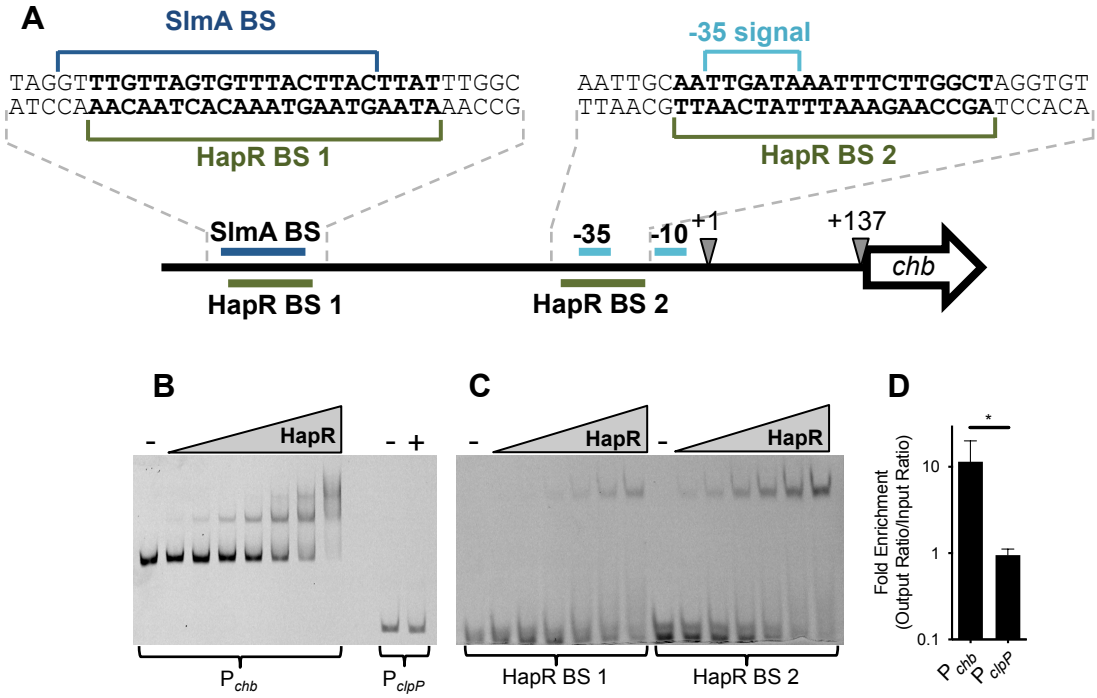

Figure 3. *HapR binds P_{chb} in vitro and in vivo.* **A**) Promoter map of P_{chb} highlighting putative HapR binding sites (BSs). Other sites required for P_{chb} activation (the SlmA BS and the -35 and -10 signals) are highlighted. The exact sequences of the region containing the HapR BSs (bolded), the SlmA BS, and the -35 signal are shown. The transcriptional start site (+1) and the translational start site (+137) are also shown. **B**) A representative EMSA using HapR and Cy5-labeled DNA probes of the indicated promoters. The P_{chb} probe was incubated with (from left to right) 0 nM (-), 12.5 nM, 25 nM, 50 nM, 100 nM, 200 nM, 400 nM, or 800 nM purified HapR. The P_{clpP} probe was incubated with 0 nM (-) or 800 nM HapR (+). **C**) A representative EMSA using HapR and 32 bp Cy5-labeled probes encompassing each of the putative HapR binding sites within the *chb* promoter (exact probe sequences are shown in **A**). The 32 bp probes were incubated with (from left to right) 0 nM (-), 100 nM, 200 nM, 400 nM, 800 nM, 1.6 µM, or 3.2 µM purified HapR. **D**) ChIP-qPCR assays showing enrichment of the indicated promoters relative to *rpoB*, a reference locus that HapR does not bind to. Data are from five independent biological replicates and shown as the mean ± SD. Statistical comparisons were made by Student's t-test. *, p = 0.0240.

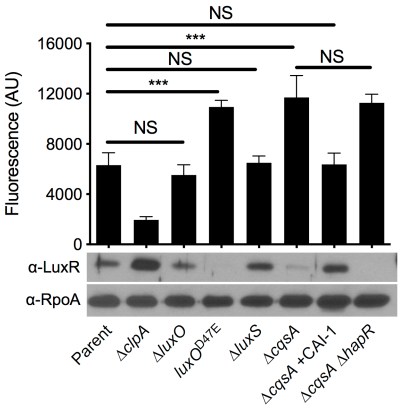

Figure 4. *Quorum sensing regulates expression of P_{chb} through the cholera-specific autoinducer CAI-1*. **A**) Model of QS regulation in *V. cholerae*. There are four sensor kinases that contribute to canonical QS in *V. cholerae* to regulate HapR production: LuxQ, CqsS, VpsS, and CqsR. The signals for VpsS and CqsR are unknown. LuxPQ senses the interspecies autoinducer AI-2 and CqsS senses the *V. cholerae*-specific autoinducer CAI-1. AI-2 is produced by the LuxS synthase and CAI-1 is produced by the CqsA synthase. (Left) At low cell density, the LuxQ and CqsS sensors act as kinases, resulting in phosphorylation of LuxO, which subsequently decreases expression of HapR. (Right) At high cell density when concentrations of AI-2 and CAI-1 are high, LuxQ and CqsS act as phosphatases, which results in dephosphorylation of LuxO, and subsequent activation of HapR expression. **B**) Expression of a P_{chb}-GFP reporter and HapR protein levels were determined in the indicated strains. The parent strain contains a P_{chb}-GFP reporter and a Δ*cbp* mutation. A representative western blot is shown below the bars to indicate the protein levels for HapR and RpoA (a loading control) in the corresponding strains. An antibody against LuxR, which has 72% identity and 86% similarity to HapR, is cross-reactive with HapR and so was used to detect HapR protein levels. Statistical comparisons were made by one-way ANOVA with Tukey's post-test. NS, not significant. ***, $p < 0.001$. The P_{chb}-GFP fluorescence data for "Parent" and "Δ*clpA*" are identical to the data presented in **Fig. 1** and were included here to ease comparisons.

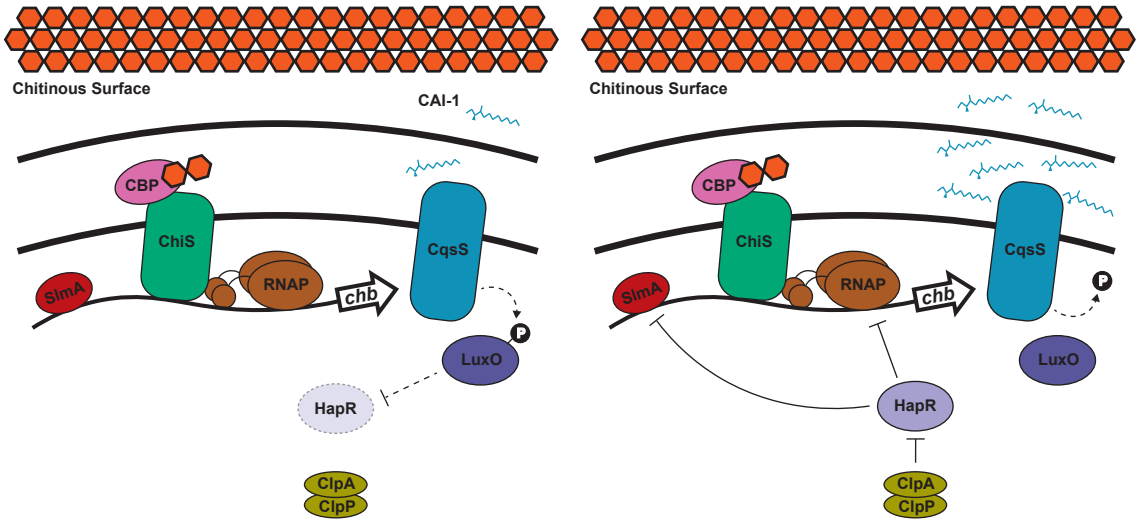

Figure 5. *Model of quorum sensing regulation of chitobiose utilization genes in V. cholerae*. When *V. cholerae* grows on a chitinous surface, the periplasmic chitin binding protein (CBP) binds to chitin oligosaccharides. This de-represses ChiS, which can then activate expression of the chitobiose utilization operon (*chb*) through recruitment of RNA Polymerase (RNAP) (10). Binding of SlmA to P_{chb} is also required for transcriptional activation (11). **A**) At low CAI-1 concentrations, the CqsS sensor indirectly (dashed line) promotes LuxO phosphorylation, which indirectly blocks HapR expression. In this state, P_{chb} is maximally expressed. **B**) At high CAI-1 concentrations, the CqsS sensor indirectly dephosphorylates LuxO, which results in indirect activation of HapR expression. HapR then exerts a repressive effect on P_{chb} by decreasing expression of this locus ~2-fold in the presence of the ClpAP protease machine. If HapR is not degraded by ClpAP, its repressive effect can result in a ~7-fold decrease in P_{chb} expression. The mechanism of HapR repression may be through occluding binding of SlmA or RNAP to P_{chb}.

974 **Table 1.** *Strains used in this study.*

Strain Designation	Reference in Manuscript	Genotype	Reference
SAD 030	*V. cholerae* E7946 WT; parent for all other E7946 strains; Fig. S2 Parent	*V. cholerae* E7946 O1 El Tor	(50)
SAD 2825	Activator screen strain	*V. cholerae* E7946 ΔVC1807::P_{chb}-mCherry, Kan^R; P_{chb}-*lacZ*, $Spec^R$; ΔVCA0692::*chiS*, Tm^R; Δ3' *cbp*, pDL1086 Cm^R $Carb^R$	This study
SAD 2826	Δ*clpA* counter-screen strain	*V. cholerae* E7946 ΔVC1807::P_{chb}-mCherry, Kan^R; P_{chb}-*lacZ*, $Spec^R$; Δ*clpA*; Δ*cbp*::Tm^R; pDL1086, Cm^R $Carb^R$	This study
SAD 1309	Fig. 1 & 4 Parent; Fig. S5 HapR WT	*V. cholerae* E7946 Δ*lacZ*:: P_{chb}-GFP, Kan^R; Δ*cbp*::$Spec^R$	(11)
SAD 2827	Fig. 1 & 4 Δ*clpA*	*V. cholerae* E7946 Δ*lacZ*:: P_{chb}-GFP, Kan^R; Δ*clpA*::$Carb^R$; Δ*cbp*::$Spec^R$	This study
SAD 2828	Fig. 1 Δ*clpP*	*V. cholerae* E7946 Δ*lacZ*:: P_{chb}-GFP, Kan^R; Δ*clpP*::$Carb^R$; Δ*cbp*::Tm^R	This study
SAD 2829	Fig. 1 Δ*clpAP*	*V. cholerae* E7946 Δ*lacZ*:: P_{chb}-GFP, Kan^R; Δ*clpA*::$Carb^R$; Δ*clpP*::Tm^R; Δ*cbp*::$Spec^R$	This study
SAD 2830	Fig. 1 Δ*clpS*	*V. cholerae* E7946 Δ*lacZ*:: P_{chb}-GFP, Kan^R; Δ*clpS*::$Carb^R$; Δ*cbp*::Tm^R	This study
SAD 2831	Fig. 1 Δ*clpX*	*V. cholerae* E7946 Δ*lacZ*:: P_{chb}-GFP, Kan^R; Δ*clpX*::$Carb^R$; Δ*cbp*::Tm^R	This study
SAD 2832	Fig. 1 Δ*lonA*	*V. cholerae* E7946 Δ*lacZ*:: P_{chb}-GFP, Kan^R; Δ*lonA*::Tm^R; Δ*cbp*::$Carb^R$	This study
SAD 2833	Fig. 1 Δ*hapR* Δ*clpA*	*V. cholerae* E7946 Δ*lacZ*:: P_{chb}-GFP, Kan^R; Δ*hapR*::$Spec^R$; Δ*clpA*::$Carb^R$; Δ*cbp*::Tm^R	This study
SAD 2834	Fig. 1 Δ*hapR*	*V. cholerae* E7946 Δ*lacZ*:: P_{chb}-GFP, Kan^R; Δ*hapR*::$Spec^R$; Δ*cbp*::$Carb^R$	This study
SAD 2835	Fig. 2 Parent	*V. cholerae* E7946 Δ*lacZ*::P_{chb}-mCherry, Kan^R; ΔVCA0692::P_{const2}-GFP, $Spec^R$	This study
SAD 2836	Fig. 2 Δ*hapR*	*V. cholerae* E7946 Δ*lacZ*::P_{chb}-mCherry, Kan^R; ΔVCA0692::P_{const2}-GFP, $Spec^R$; Δ*hapR*::Cm^R	This study
SAD 2837	Fig. 2 Δ*cbp* & Fig. S3 E7946 Parent	*V. cholerae* E7946 Δ*lacZ*::P_{chb}-mCherry, Kan^R; ΔVCA0692::P_{const2}-GFP, $Spec^R$; Δ*cbp*::Tm^R	This study
SAD 2838	Fig. 2 Δ*hapR* Δ*cbp* & Fig. S3 E7946 Δ*hapR*	*V. cholerae* E7946 Δ*lacZ*::P_{chb}-mCherry, Kan^R; ΔVCA0692::P_{const2}-GFP, $Spec^R$; Δ*hapR*::Cm^R; Δ*cbp*::Tm^R	This study
SAD 2839	Fig. 3 ChIP strain and Fig. S5 1x FLAG-HapR	*V. cholerae* E7946 Δ*lacZ*::P_{chb}-GFP, Kan^R; 1x FLAG-*hapR*; Δ*cbp*::Tm^R	This study
SAD 2840	Fig. 4 Δ*luxO*	*V. cholerae* E7946 Δ*lacZ*::P_{chb}-GFP, Kan^R; Δ*luxO*::$Spec^R$; Δ*cbp*::$Carb^R$	This study
SAD 2841	Fig. 4 $luxO^{D47E}$	*V. cholerae* E7946 Δ*lacZ*::P_{chb}-GFP, Kan^R; $luxO^{D47E}$; Δ*cbp*::$Spec^R$	This study
SAD 2842	Fig. 4 Δ*luxS*	*V. cholerae* E7946 Δ*lacZ*::P_{chb}-GFP, Kan^R; Δ*luxS*::Cm^R; Δ*cbp*::$Spec^R$	This study
SAD 2843	Fig. 4 Δ*cqsA*	*V. cholerae* E7946 Δ*lacZ*::P_{chb}-GFP, Kan^R; Δ*cqsA*::Tm^R; Δ*cbp*::$Spec^R$	This study
SAD 2844	Fig. 4 Δ*cqsA* Δ*hapR*	*V. cholerae* E7946 Δ*lacZ*::P_{chb}-GFP, Kan^R; Δ*cqsA*::Tm^R; Δ*hapR*::Cm^R; Δ*cbp*::$Spec^R$	This study

SAD 306	*V. cholerae* A1552 WT; parent for all other A1552 strains	*V. cholerae* A1552 O1 El Tor	(51)
SAD 2908	*E. coli* strain used to mate pMMB tfoX-qstR into complementation strains used in Fig. S1	*E. coli* S17 harboring pMMB67EH *tfoX qstR*, Cm^R	This study
SAD 2909	Fig. S1 Δ*hapR* P_{hapR}-*hapR*	*V. cholerae* E7946 Δ*lacZ*::P_{chb}-GFP Kan^R; Δ*hapR*::$Spec^R$; Δ*cbp*::$Carb^R$; ΔVCA0692::P_{hapR}-*hapR*, Tm^R	This study
SAD 2910	Fig. S1 Δ*hapR* Δ*clpA* P_{hapR}-*hapR*	*V. cholerae* E7946 Δ*lacZ*::P_{chb}-GFP Kan^R; Δ*hapR*::$Spec^R$; Δ*clpA*::$Carb^R$; Δ*cbp*::Tm^R; ΔVCA0692::P_{hapR}-*hapR*, Zeo^R	This study
SAD 2911	Fig. S1 Δ*clpA* P_{clpSA}-*clpSA*	*V. cholerae* E7946 Δ*lacZ*::P_{chb}-GFP Kan^R; Δ*clpA*::$Carb^R$; Δ*cbp*::$Spec^R$; ΔVCA0692::P_{clpSA}-*clpSA*, Tm^R	This study
SAD 2912	Fig. S2 Δ*hapR*	*V. cholerae* E7946 Δ*hapR*::Cm^R	This study
SAD 2845	Fig. S3 A1552 Parent	*V. cholerae* A1552 ΔVCA0692::P_{const2}-GFP, $Spec^R$; Δ*lacZ*::P_{chb}-mCherry, Kan^R; Δ*cbp*::Tm^R	This study
SAD 2846	Fig. S3 A1552 Δ*hapR*	*V. cholerae* A1552 ΔVCA0692::P_{const2}-GFP, $Spec^R$; Δ*lacZ*::P_{chb}-mCherry, Kan^R; Δ*hapR*::Cm^R; Δ*cbp*::Tm^R	This study
SAD 2847	Fig. S4 WT *lacZ*$^+$	*V. cholerae* E7946 ΔVC1807::Cm^R; ΔVC0995	This study
SAD 2848	Fig. S4 WT Δ*lacZ*	*V. cholerae* E7946 Δ*lacZ*::$Spec^R$; ΔVC1807::Cm^R; ΔVC0995	This study
SAD 2849	Fig. S4 Δ*hapR* Δ*lacZ*	*V. cholerae* E7946 Δ*lacZ*::$Spec^R$; ΔVC1807::Cm^R; ΔVC0995; Δ*hapR*::Tm^R	This study
JDN 71	Fig. 3B, 3C purified HapR	*E. coli* BL21(DE3) harboring pET28b-*6XHis-hapR*, Kan^R	This study

975
976
977
978

979 **Table 2.** *Primers used in this study.*

Primers for Inverse PCR		
Primer	**Sequence**	**Description**
BBC 244	CCCGGGATCCTGTGTGAAATTGTTATCCGC	Tn10-specific primer for Inverse PCR
BBC 434	GTGTGGGCACTCGACATATGACAAG	Tn10-specific primer for Inverse PCR
Primers for Reporter Constructs		
Primer	**Sequence**	**Description**
ABD 332	GGCTGAACGTGGTTGTCGAAAATGAC	Δ*lacZ* F1 (Up Arm)
BBC 219	GTTTATTTTTGTCGACTGTACAGCGTTTAAATAGAGGTCGATATTGACCC	Δ*lacZ* R1 (Up Arm)
ABD 342	ATTTTTCAGTTGGCCTACAATGCTTTCC	ΔVC1807 F1 (Up Arm)
BBC 719	CACCATACCCACGCCGAAACAAGGATTTTGAATTAAACGTTTCATTAGTC	ΔVC1807 R1 (Up Arm)
BBC 218	CGCTGTACAGTCGACAAAAATAAAC	Kan^R F (Middle Arm)
BBC 262	TACCGAGGACGCGAAGCTG	Kan^R R (Middle Arm)
BBC 266	CAGCTTCGCGTCCTCGGTAGAATAAAGCAATCCGCAAGCG	P_{chb} F (Middle Arm)
BBC 267	CCCGGGATCCTGTGTGAAATTGAGTTGCTTTCATTTCACTAATGG	P_{chb} R (Middle Arm)
BBC 732	ctcaagccgaggagtaaagaagAGTTGCTTTCATTTCACTAATGG	P_{chb} fuse to *lacZ* R (Middle Arm)
BBC 252	CAATTTCACACAGGATCCCGGGAGGAGGTAACGTAATGCGTAAAGGAGAAGAAC	GFP F (Middle Arm)
BBC 254	tgtaggctggagctgcttcTTAGTTGTATAGTTCATCCATGCC	GFP R (Middle Arm)
BBC 1356	TTGTTTCGGCGTGGGTATGGTGCGCTGTACAGTCGACAAAAATAAAC	mCherry F (Middle Arm)
BBC 206	tgtaggctggagctgcttcttacttgtacagctcgtccatg	mCherry R (Middle Arm)
ABD 785	CTTCTTTACTCCTCGGCTTGAG	P_{chb} stitch to *lacZ* F (Down Arm)
ABD 255	gaagcagctccagcctacaCCACAATAAGCCAGAGAGCCTTAAG	Δ*lacZ* F2 (Down Arm)
ABD 256	CCCAAATACGGCAACTTGGCG	Δ*lacZ* R2 (Down Arm)
ABD 341	gaagcagctccagcctacaTAGTCGAAAATAAAAAAAAGAGGCTCGCCTC	ΔVC1807 F2 (Down Arm)
ABD 345	CTTGCTAACCGTTGGTGTTACCAGC	ΔVC1807 R2 (Down Arm)
BBC 3083	tggataactttacgggcatgcataaggctcgtataatatattcagggagaccacaacggtttccctctacaaataattttgtttaactttCAATTTCACACAGGATCCCGGG	P_{const2} F
BBC 3082	ttatacgagccttatgcatgcccgtaaagttatccagcaaccactcatagacctagggcagcagataggacgacgtggtgttagctgtgCTCATTAGGCACCCCAGGC	P_{const2} R
Primers for SOE deletion, FLAG fusions, and point mutants		
Primer	**Sequence**	**Description**
BBC 742	attccggggatccgtcgacCTGCAGTTCagaagcagctccagcctaca	MiniFRT F
BBC 743	tgtaggctggagctgcttctGAACTGCAGgtcgacggatccccggaat	MiniFRT R

ABD 123	ATTCCGGGGATCCGTCGAC	Kan^R, Spec^R, Carb^R, Cm^R or Tm^R cassette F
ABD 124	TGTAGGCTGGAGCTGCTTC	Kan^R, Spec^R, Carb^R, Cm^R or Tm^R cassette R
ABD 796	TTAGAATCTGCGCCAGAAGCG	Δ*cbp* F1 (Up Arm)
ABD 797	gtcgacggatccccggaatCATAGCTGTTCCTTACTAGTTGC	Δ*cbp* R1 (Up Arm)
BBC 920	gtcgacggatccccggaatGCTCATCAGGTCGTCAGCC	Δ3' *cbp* R1 (Up Arm)
ABD 798	gaagcagctccagcctacaGTACTGGATCTGAAACCAGTTAAG	Δ*cbp* F2 (Down Arm)
ABD 799	GTATTGCGGAATGACCAGCATG	Δ*cbp* R2 (Down Arm)
BBC 2755	TTACCCCTAAGTCGGCGAGC	ΔVC0995 F1 (Up Arm)
BBC 2756	gtcgacggatccccggaatAATATTCACCTTAAGTTCCCCC	ΔVC0995 R1 (Up Arm)
BBC 2757	gaagcagctccagcctacaCTGCCTTAATCGAGTTTAAACCC	ΔVC0995 F2 (Down Arm)
BBC 2758	GCACCACGATAGCAATAAGC	ΔVC0995 R2 (Down Arm)
CAK 407	GCTACGCACTGCCAAATTACC	Δ*clpA* or Δ*clpS* F1 (Up Arm)
CAK 408	gtcgacggatccccggaatAAGCATAAGGCCTCCTTAAGGAAC	Δ*clpA* R1 (Up Arm)
CAK 409	gaagcagctccagcctacaCACTAGACATCTCACAATACGC	Δ*clpA* F2 (Down Arm)
CAK 410	CCGCTAACATCTCAGGACTG	Δ*clpA* or Δ*clpS* R2 (Down Arm)
CKP 449	TGCTCGGTTTTGATCCGTTC	Δ*clpP* or Δ*clpX* F1 (Up Arm)
CKP 450	gtcgacggatccccggaatGGGCGACATTGCATTTTTTTC	Δ*clpP* R1 (Up Arm)
CKP 451	gaagcagctccagcctacaGGCGAGTAAGCTCGTAATTG	Δ*clpP* F2 (Down Arm)
CKP 454	GTCAAACTAGAAACCAGCGC	Δ*clpP* or Δ*clpX* R2 (Down Arm)
CKP 447	gtcgacggatccccggaatTTTACTCATGACACTTCAATATTTG	Δ*clpS* R1 (Up Arm)
CKP 448	gaagcagctccagcctacaCAAGCTTAAACTTGCCGGGC	Δ*clpS* F2 (Down Arm)
CKP 452	gtcgacggatccccggaatGTCTGTCATTCGCTAACCTC	Δ*clpX* R1 (Up Arm)
CKP 453	gaagcagctccagcctacaGCGGAGTAATCTCAAGCAAC	Δ*clpX* F2 (Down Arm)
CKP 489	TTGACGCTCTGAAAGCAGAAG	Δ*lonA* F1 (Up Arm)
CKP 490	gtcgacggatccccggaatCAAGTTCATATTTTTCTCTCTTCCG	Δ*lonA* R1 (Up Arm)
CKP 491	gaagcagctccagcctacaGATGCATAGCAAAAATAAGTAAATC	Δ*lonA* F2 (Down Arm)
CKP 492	CGAAGAATTATAAGTGCAAAGGC	Δ*lonA* R2 (Down Arm)
BBC 422	ACGTTCAATAACCAGAATGTTGG	Δ*hapR* F1 (Up Arm)
BBC 423	gtcgacggatccccggaatTTTTCGATTGATGCGTCCATAG	Δ*hapR* R1 (Up Arm)
CKP 511	GTCtttgtcatcgtcatccttataatcCATAGGGGTATATCCTTGCC	*1x FLAG-hapR* R1 (Up Arm)

BBC 408	gaagcagctccagcctacaAACTAGTTTCTTGGGCAGCACAA	Δ*hapR* F2 (Down Arm)
CKP 510	ATGgattataaggatgacgatgacaaaGACGCATCAATCGAAAAACG	*1x FLAG-hapR* F2 (Down Arm)
BBC 409	GTTCATAATGATTTCCTTGGTGCC	Δ*hapR* R2 (Down Arm)
BBC 374	TGGCAAAAAGCGAGAGAAGAAG	Δ*luxO* F1 (Up Arm)
BBC 375	gtcgacggatccccggaatCATGAGGACATATTTTGTTTTCTGC	Δ*luxO* R1 (Up Arm)
CKP 519	TCATATCTGGCAAACGTAAcTCCAGCAGGATTAAGTCAGG	*luxO*^{D47E} R1 (Up Arm)
BBC 376	gaagcagctccagcctacaTAAGCGATGAGAGAATGGATCAAC	Δ*luxO* F2 (Down Arm)
CKP 518	TGACTTAATCCTGCTGGAgTTACGTTTGCCAGATATGACG	*luxO*^{D47E} F2 (Down Arm)
BBC 377	TCACACCCGAATTTCCATCATGC	Δ*luxO* R2 (Down Arm)
CKP 554	GTCTCTTAGCCGAGGTACTG	Δ*cqsA* F1 (Up Arm)
CKP 555	gtcgacggatccccggaatCTTGTTCATCGCAATATATCCTAG	Δ*cqsA* R1 (Up Arm)
CKP 556	gaagcagctccagcctacaTTTCGTTAAATGCATAAATAACAAAAAC	Δ*cqsA* F2 (Down Arm)
CKP 557	AGTTGGAACCACTTCTTGTC	Δ*cqsA* R2 (Down Arm)
CKP 549	TACAACTGCTTGGCACGC	Δ*luxS* F1 (Up Arm)
CKP 550	gtcgacggatccccggaatTGGCATTTCCTTTCTCCC	Δ*luxS* R1 (Up Arm)
CKP 551	gaagcagctccagcctacaCACTAAGTCGGTTCTGTAAACG	Δ*luxS* F2 (Down Arm)
CKP 552	TTCTTAGCGTGATCAATTGC	Δ*luxS* R2 (Down Arm)
ABD 334	AGTGCTCCGGACTCTTTGCTCTG	Δ*lacZ* F1 (Up Arm)
ABD 254	gtcgacggatccccggaatCATCCCTCAAGCCGAGGAGTAAAG	Δ*lacZ* R1 (Up Arm)
ABD 255	gaagcagctccagcctacaCCACAATAAGCCAGAGAGCCTTAAG	Δ*lacZ* F2 (Down Arm)
ABD 256	CCCAAATACGGCAACTTGGCG	Δ*lacZ* R2 (Down Arm)
ABD 725	GAAGCAGCTCCAGCCTACA	Detect F for all deletions
BBC 082	gtcgacggatccccggaatCATAACTTACACCTTACTCACCCAG	Δ*cbp* detect R
CAK 411	TTGTTTGGTGCGATTATTGG	Δ*clpA* detect R
CKP 464	TTGGCAGAACATCTTTGATC	Δ*clpP* detect R
CKP 463	AAAGTATCCAGCTCACGGCG	Δ*clpS* detect R
CKP 465	CCATGTGTGGATAGACAACC	Δ*clpX* detect R
CKP 493	CAGTGCCACTTGGTCACCTG	Δ*lonA* detect R
BBC 410	TAAATGGGGCTTGGAGAATTTAG	Δ*hapR* detect R
BBC 1911	CGTAATCAAACTGCGAAAGTG	Δ*luxO* detect R
CKP 558	AATTCGTAACTCTGAGCATG	Δ*cqsA* detect R
CKP 553	TGGACCACGAACCTTAAACG	Δ*luxS* detect R
BBC 2759	TTGTCAGAAAGCGTTTCTGC	ΔVC0995 detect R
ABD 399	AACTGATGGCAGAAAAAGCCACTCAG	Δ*lacZ* detect R
BBC 993	ttgattataaggatgacgatgac	*1x FLAG* detect F
ABD 846	CATAAACATGTTTCTGATCAGCAG	*1x FLAG-hapR* detect R
BBC 380	GCCAATAGAATGAGTCTATTGGCTG	*luxO*^{D47E} detect F
CKP 520	TCATATCTGGCAAACGTAgc	*luxO*^{D47E} detect R
Primers for EMSA probes		

Primer	Sequence	Description
BBC 744	cagcttcgcgtcctcggtaCGCAAATATAACTCAGGCAAAG	P_{chb} F
CKP 072	cccgggatcctgtgtgaaattgCTTTGGCAGGAGTAAGAAAACACCTAG	P_{chb} R
CKP 865	TAAGCAAACTGTAGCGTAGAAG	P_{clpP} F
CKP 866	TGCATTTTTTTCTTGGTAGC	P_{clpP} R
CKP 504	GCCAAATAAGTAAGTAAACACTAACAAACCTA	HapR BS 1 F
CKP 505	TAGGTTTGTTAGTGTTTACTTACTTATTTGGC	HapR BS 1 R
CKP 506	AATTGCAATTGATAAATTTCTTGGCTAGGTGT	HapR BS 2 F
CKP 507	ACACCTAGCCAAGAAATTTATCAATTGCAATT	HapR BS 2 R
Primers for qPCR and qRT-PCR		
Primer	**Sequence**	**Description**
BBC 989	GCATCTAGGTTTTGACGTTTTTAACG	P_{chb} amplify F
BBC 990	AACACTCTCCAAGACCTACCTC	P_{chb} amplify R
ABD 132	CTGTCTCAAGCCGGTTACAA	*rpoB* amplify F
ABD 133	TTTCTACCAGTGCAGAGATGC	*rpoB* amplify R
CKP 865	TAAGCAAACTGTAGCGTAGAAG	P_{clpP} amplify F
CKP 867	TCGTATGAACGCTCACCACG	P_{clpP} amplify R
Primers for purification vector		
Primer	**Sequence**	**Description**
JDN 92	agcagcggcctggtgccgcgcggcagcCatatggacgcatcaatcgaaaaa	Cloning *6X-His-hapR* into pET28b vector via IDA, F
JDN 93	tcagtggtggtggtggtggtgCTCGAGctagttcttatagatacacagcatattgagg	Cloning *6X-His-hapR* into pET28b vector via IDA, R
JDN 22	CTCGAGcaccaccaccacca	Amplify pET28b vector backbone for IDA, F
JDN 23	atGgctgccgcgcggcacca	Amplify pET28b vector backbone for IDA, R
Primers for complementation constructs		
BBC 832	GCTTTTTGCTACAACGACCG	ΔVCA0692 F1 for Up arm
BBC 828	CACCATACCCACGCCGAAACAACAGTGATGTAGCGAATCGGAC	ΔVCA0692 R1 for Up arm
BBC 243	TTGTTTCGGCGTGGGTATGGTG	Tm^R or Zeo^R F for Middle arm
BBC 647	tttttctatttctgaatcgattcatacgaCTCATTAGGCACCCCAGGC	Tm^R F or Zeo^R for Middle arm
CKP 948	tcgtatgaatcgattcagaaatagaaaaaACCATTCTCGTTGTGTTGGG	P_{hapR}-*hapR* F for Middle arm
BBC 729	tgtaggctggagctgcttcCTAGTTCTTATAGATACACAGCATATTG	P_{hapR}-*hapR* R for Middle arm
CKP 949	tcgtatgaatcgattcagaaatagaaaaaCCCTCATGCATTTTATAACTG	P_{clpSA}-*clpSA* F for Middle arm
CKP 950	tgtaggctggagctgcttcCTAGTGGACCACCTCTTCGC	P_{clpSA}-*clpSA* R for Middle arm
BBC 830	gaagcagctccagcctacaGTTGAGTTGGATGCAGCACC	ΔVCA0692 F2 for Down arm
BBC 834	CACAATTTCTCGCTTAAAATGTCC	ΔVCA0692 R2 for Down arm
CKP 509	gcaggtggagcaggtggaGACGCATCAATCGAAAAACG	ΔVCA0692::P_{hapR}-*hapR* detect F

BBC 1101	CAGACGTACTATTAACAGGACTGAC	ΔVCA0692::P_{hapR}-*hapR* detect R
CKP 235	gtcgacggatccccggaatCAAATATATCCTCCTCACTATTTTGATTAG	ΔVCA0692::P_{clpSA}-*clpSA* detect F
CKP 447	gtcgacggatccccggaatTTTACTCATGACACTTCAATATTTG	ΔVCA0692::P_{clpSA}-*clpSA* detect R

980

Supplemental Information for

Species-specific quorum sensing represses the chitobiose utilization locus in *Vibrio cholerae*

Catherine A. Klancher, Jane D. Newman, Alyssa S. Ball, Julia C. van Kessel, and Ankur B. Dalia*

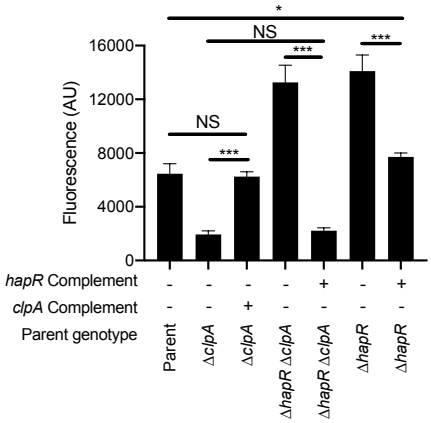

Figure S1. *Complementation of ΔhapR and ΔclpA mutant strains.* Expression of a P_{chb}-GFP transcriptional reporter was determined in the indicated strains. The parent strain contained a chromosomally-encoded P_{chb}-GFP reporter and a Δ*cbp* mutation. Strains were complemented with a chromosomally-encoded single copy of the indicated gene driven by its native promoter at an ectopic site (*hapR* or *clpA* Complement). Fluorescence of cultures was determined on a plate reader from at least three independent biological replicates and is shown as the mean ± SD. Statistical comparisons were made by one-way ANOVA with Tukey's post-test. NS, not significant. *, $p = 0.0104$. ***, $p < 0.001$. The P_{chb}-GFP fluorescence data for "Δ*clpA*", "Δ*hapR* Δ*clpA*", and "Δ*hapR*" are identical to the data presented in **Fig. 1** and were included here for ease of comparison.

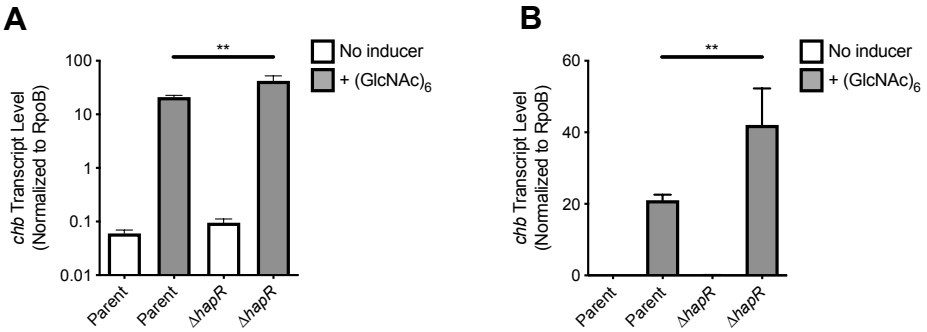

Figure S2. *HapR is a repressor of native chb expression.* The indicated strains were induced with sterile water (no inducer) or chitin oligosaccharides (+ $(GlcNAc)_6$), then assessed for *chb* transcript abundance by qRT PCR. The parent strain used was *V. cholerae* E7946 WT. Data are shown on **A**) a log scale or **B**) a linear scale. The latter plot helps accentuate that deletion of *hapR* results in a two-fold increase in native *chb* transcripts in response to chitin oligosaccharides, which is similar to what is observed using transcriptional reporters. Data are from at least three independent biological replicates and is shown as the mean ± SD. Statistical comparisons were made by one-way ANOVA with Tukey's post-test. **, $p = 0.0064$.

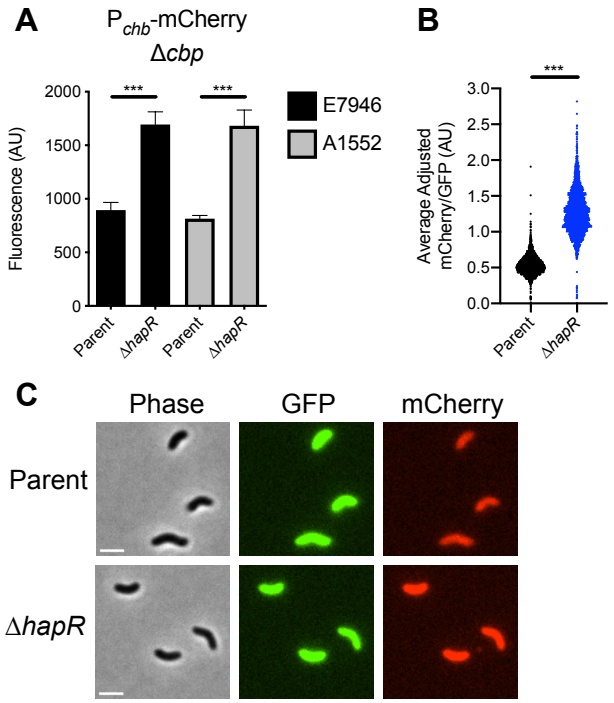

Figure S3. *HapR is a repressor of P_{chb} in V. cholerae E7946 and V. cholerae A1552.* **A**) Expression of a P_{chb}-mCherry reporter was determined in the indicated mutant strains. Each respective parent strain contained a P_{chb}-mCherry reporter and a Δ*cbp* mutation to activate ChiS. **B**) Scatter plot showing the relative expression of a P_{chb}-mCherry reporter in the indicated *V. cholerae* A1552 strains that have *cbp* intact when using chitin oligosaccharides to induce cells. The parent strain background contains both a P_{chb}-mCherry reporter, a P_{const2}-GFP construct (which exhibits constitutive GFP expression), and *cbp* intact. n = 2189 for Parent; n = 2164 for Δ*hapR.* Data shown are from two independent biological replicates. **C**) Representative images of *V. cholerae* A1552 strains analyzed in **B**. Scale bar = 2 µm. Statistical comparisons in **A** were made using a one way ANOVA with Tukey's post test and in **B** were made using Student's t-test. ***, $p < 0.001$.

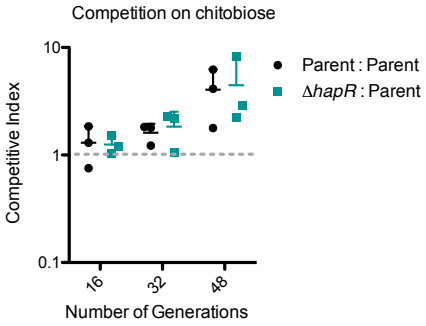

Figure S4. A Δ*hapR mutant does not have a fitness advantage for growth on chitobiose.* The indicated *V. cholerae* strains were mixed and co-cultured in M9 minimal media supplemented with 0.2% chitobiose + 10 μM CAI-1 and grown for the indicated number of generations. Each data point represents an independent biological replicate.

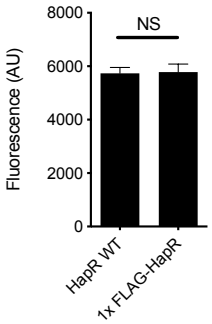

Figure S5. *N-terminally FLAG-tagged HapR is functional for regulation of P_{chb}.* Strains expressing the indicated HapR allele at the native locus were assessed for expression of a P_{chb}-GFP reporter. Both strains also harbored a Δ*cbp* deletion to activate ChiS. Statistical comparisons were made using Student's t-test. NS, not significant.

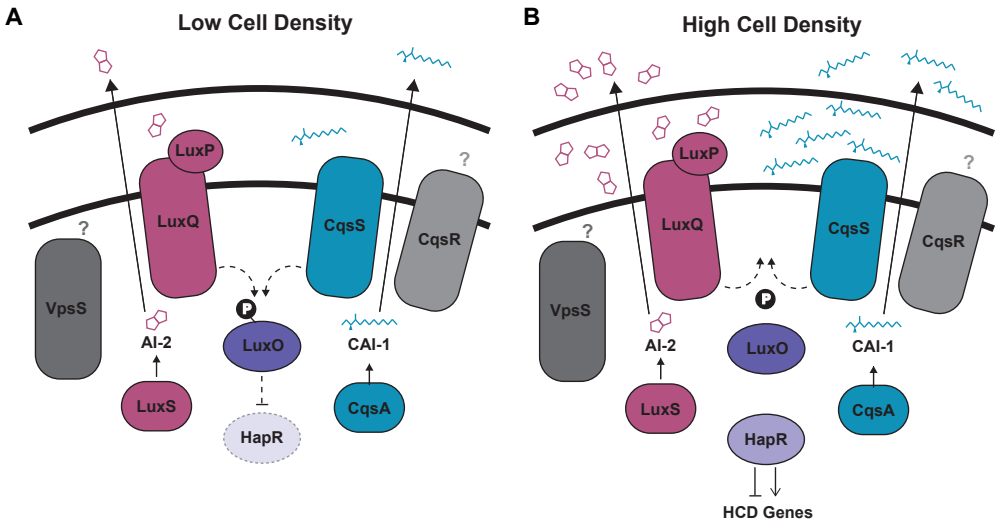

Figure S6. Model of quorum sensing regulation in *V. cholerae*. There are four parallel sensor kinases that contribute to QS in *V. cholerae*: LuxQ, CqsS, VpsS, and CqsR. The signals for VpsS and CqsR are unknown. LuxPQ senses the interspecies autoinducer AI-2 and CqsS senses the *V. cholerae*-specific autoinducer CAI-1. AI-2 is produced by the LuxS synthase and CAI-1 is produced by the CqsA synthase. (**A**) At low cell density, the LuxQ and CqsS sensors act as kinases, resulting in phosphorylation of LuxO, which subsequently decreases expression of HapR. (**B**) At high cell density, LuxQ and CqsS act as phosphatases, which results in dephosphorylation of LuxO, and subsequent activation of HapR expression. Dashed lines indicate indirect effects of one protein on another.

Table S1. *Other hits from P_{chb} activator screen and ΔclpA counter-screen.*

Activator or Δ*clpA* counter-screen?	Gene	VC gene designation	Putative function	Number of unique insertions
Activator	*treC*	VC0911	Trehalose-6-phosphate hydrolase	5
Activator	*cyaA*	VC0122	Adenylate cyclase	1
Δ*clpA* counter-screen	*nagC*	VC0993	GlcNAc transcriptional repressor protein	4
Δ*clpA* counter-screen	*cytR*	VC2677	Cytidine repressor protein	1